Experimental validation of Monte Carlo dosimetry for therapeutic beta emitters with radiochromic film in a 3D printed phantom

Benjamin Van[1], Yuni K. Dewaraja[1], Jeremy T. Niedbala[1], Gerrid Rosebush[1], Matthew Kazmierski[1], David Hubers[1], Justin K. Mikell[2,4*], Scott J. Wilderman[3*]

[1] Department of Radiology, Michigan Medicine, Ann Arbor, MI, 48109, USA

[2]Department of Radiation Oncology, Michigan Medicine, Ann Arbor, MI, 48109, USA

[3]Department of Nuclear Engineering and Radiologic Sciences, University of Michigan, Ann Arbor, MI, 48109, USA

[4]Department of Radiation Oncology, Washington University in St. Louis, St. Louis, MO, 63110, USA

*Co-senior Authorship

Corresponding Author: Yuni K. Dewaraja

Email: **yuni@umich.edu**

Mail: Yuni Dewaraja, PhD

Professor

Division of Nuclear Medicine

Department of Radiology

University of Michigan

1301 Catherine

2276 Med Sci 1/SPC 5610

Ann Arbor, MI 48109

Running Title: Therapeutic beta emission dosimetry

Abstract

Purpose: Validation of dosimetry software, such as Monte Carlo (MC) radiation transport codes used for patient-specific absorbed dose estimation, is critical prior to their use in clinical decision making. However, direct experimental validation in the clinic is generally not performed for low/medium-energy beta emitters used in radiopharmaceutical therapy (RPT) due to the challenges of measuring energy deposited by short-range particles. Our objective was to design a practical phantom geometry for radiochromic film (RF) based absorbed dose measurements of beta-emitting radionuclides and perform experiments to directly validate our in-house developed Dose Planning Method (DPM) MC code dedicated to internal dosimetry.

Methods: The experimental setup was designed for measuring absorbed dose from beta emitters that have a range sufficiently penetrating to ~200µm in water as well as to capture any photon contributions to absorbed dose. Assayed ^{177}Lu and ^{90}Y liquid sources, 13 - 450MBq estimated to deliver 0.5-10Gy to the sensitive layer of the RF, were injected into the cavity of two 3D printed half-cylinders that had been sealed with 12.7µm or 25.4µm thick Kapton Tape. A 3.8x6cm strip of GafChromic EBT3 RF was sandwiched between the two taped half-cylinders. After a 2-48hr exposures, films were retrieved and wipe tested for contamination. Absorbed dose to the RF was measured using a commercial triple-channel dosimetry optimization method and a calibration generated via 6MV photon beam. Profiles were analyzed across the central 1cm^2 area of the RF for validation. Eleven experiments were completed with ^{177}Lu and nine with ^{90}Y both in saline and a bone equivalent solution. Depth dose curves were generated for ^{177}Lu and ^{90}Y stacking multiple RF strips between a single filled half-cylinder and an acrylic backing. All experiments were modeled in DPM to generate voxelized MC absorbed dose estimates. We extended our study to benchmark general purpose MC codes MCNP6 and EGSnrc against the experimental results as well.

Results: A total of 20 experiments showed that both the 3D printed phantoms and the final absorbed

50   dose values were reproducible. The agreement between the absorbed dose estimates from the RF

measurements and DPM was on average -4.0% (range -10.9% to 3.2%) for all single film [177]Lu

experiments and was on average -1.0% (range -2.7% to 0.7%) for all single film ^{90}Y experiments.

Absorbed depth dose estimates by DPM agreed with RF on average 1.2% (range -8.0% to 15.2%) across

all depths for ^{177}Lu and on average 4.0% (range -5.0% to 9.3%) across all depths for [90]Y. DPM absorbed

55   dose estimates agreed with estimates from EGSnrc and MCNP across the board, within 4.7% and within

3.4% for ^{177}Lu and ^{90}Y respectively, for all geometries and across all depths. MC showed that absorbed

dose to RF from betas was greater than 92% of the total (betas + other radiations) for ^{177}Lu, indicating

measurement of dominant beta contribution with our design.

Conclusions: The reproducible results with a RF insert in a simple phantom designed for liquid sources

60   demonstrate that this is a reliable setup for experimentally validating dosimetry algorithms used in

therapies with beta-emitting unsealed sources. Absorbed doses estimated with the DPM MC code

showed close agreement with RF measurement and with results from two general purpose MC codes,

thereby validating the use of this algorithms for clinical RPT dosimetry.

1. Introduction

65   Nuclear medicine clinics worldwide are seeing an increase in the number of available

radiopharmaceutical therapy (RPT) options.[1,2] In addition to the well-established ^{90}Y microsphere

radioembolization (RE) for hepatic malignancies, ^{177}Lu peptide receptor radionuclide therapy (PRRT) for

neuroendocrine tumors and ^{177}Lu radioligand therapy for prostate cancer have both been recently

approved. Even new applications of ^{131}I, the classical therapy radionuclide used for decades in

70   radioiodine therapy, are emerging.[3] Alongside the rise of these new therapeutic applications comes a

renewed interest in individualized dosimetry-guided treatment planning. Accurate absorbed dose data is

also required for answering key questions that remain in the field; such as what absorbed dose-response relationships exist, what scale of dosimetry is necessary, and how spatial distribution affects outcomes.[4]

75

RPT, unlike brachytherapy or external beam radiotherapy (EBRT), commonly relies on ligand or antibody uptake in the specific cancer cell, or its close neighbors, in order to deliver a therapeutic dose of radiation. This process is inherently dependent on the cell function and distribution on a microscopic level and absorbed dose may be very non-uniform over even a couple of millimeters. This is in stark

80   contrast to EBRT where the known beam geometry covers a much larger area and any given pulse of radiation can be relativity flat across the beam. Even in brachytherapy the applicators are, relative to the size of a cell, quite large and absorbed dose approximations can be made reliably as the radiation is applied using a fixed geometry. The dependence on a non-uniform, microscopic geometry paired with short-range beta emitters in RPT increases the need to validate the absorbed dose calculation software

85   at very short distances.

Experimental absorbed dose validation for radionuclides such as ^{60}Co or ^{137}Cs used in EBRT has been widely achievable with the use of ionization chambers or thermoluminescent dosimeters (TLD),[5,6] due to the photon component being used for therapy. Radionuclides with less penetrating radiations, such as ^{177}Lu used in radiopharmaceutical therapies, require geometries and methods not commonly

90   available in commercial systems in order to directly measure the beta contribution of the absorbed dose. Low energy betas may lack the penetration distance necessary for ion chamber measurement and the liquid nature of the therapeutic agents makes contamination an additional challenge that must be overcome when using TLD's or similar detectors.

In order to directly and reliably measure the beta contribution of absorbed dose a detector must

95   be placed sufficiently close to a liquid source and have a repeatable geometry. Both RF and gel

dosimetry can fit this niche need. Gel dosimetry has been shown to be a viable measurement system

for beta particles from ^{90}Y brachytherapy seeds[7] and further investigation may be warranted in future

studies.   For a much simpler, more accessible, and less-costly measurement, film dosimetry has proven

to be a reliable method of acquiring high resolution data one plane at a time. Film dosimetry has a rich

100   history in EBRT measurements with its use in a variety of applications from megavoltage beam

commissioning to small field and in-vivo measurements.[8] Given the thin (~25 μm) active layer, high

resolution, and low dependence on absorbed dose-rate and particle energy,[9] RF can also be easily

extended for use in beta measurements relevant to RPT.

The ongoing interest in these low energy beta measurements has prompted other experiments

105   with Tiwari et. al.[11] demonstrating the use of RF measurement for ^{90}Y and ^{177}Lu at distances between

1mm and 15mm from the source, although the first 1-2mm of the film was impacted by delamination.

Their experimental configuration showed good correlation with GEANT4 Application for Tomographic

Emission (GATE)[12] MC at these distances and incorporated direct measurement of the beta, gamma, and

bremsstrahlung portions of the deposited dose. The experimental geometries and materials used for

110   their research allowed for effective measurement of absorbed dose from the ^{90}Y beta in all three of the

common clinical mediums; soft tissue, lung, and bone, however direct measurement of ^{177}Lu was

restricted to only lung equivalent materials due to the significantly shorter maximum beta range, 1.8mm

in tissue for ^{177}Lu vs 11mm[13] in tissue for [90]Y. As many of the currently used or experimental beta

emitters have low average electron energies (**Error! Reference source not found.**), the majority of their

115   absorbed dose will be deposited in path lengths shorter than 1.5mm, and a different geometry is

required for comprehensive absorbed dose validation work in this space.

Villarreal-Barajas et. al.[14] attempted RF measurement of betas at distances as short as 104μm

from a liquid [153]Sm source in an acrylic phantom.   Their experimental results showed excellent

agreement with film measurement with depths between 416μm and 832μm having agreement within

120   5%. They noted that films closer than 416μm ended up damaged during removal from the phantom,

which highlights the complexity involved in both being close to a liquid source and avoiding

contamination or other damage when doing so.

The MC method is a valuable tool for radiopharmaceutical therapy dosimetry, especially when

voxel-level estimates are of interest. As detailed in a recent publication[15], there are multiple general

125   purpose and specialized MC codes that can be used for dosimetry with explicit radiation transport using

the patient's own anatomical and emission images as well as for generating the kernels for dose kernel

convolution methods.[16,17] While direct MC radiation transport is generally accepted as superior to

convolution using MC-derived dose kernels it is computationally very demanding and can be associated

with long simulation times to obtain good statistics when general purpose codes (e.g. MCNP, EGSnrc,

130   GATE) are used.

To overcome this, the specialized MC code Dose Planning Method (DPM)[18] was originally

developed at University of Michigan for fast absorbed dose estimation in EBRT. DPM achieves its

significant speed-up over conventional MC via special transport mechanics that permits long transport

steps across heterogeneous boundaries. The accuracy of DPM at energies and geometries relevant to

135   EBRT has previously been demonstrated by benchmarking against measurements.[19,20] Since DPM was

optimized specifically for absorbed dose computations in voxel geometries, in particular, those derived

from CT-scans, it is perfectly suited for patient specific absorbed dose estimation in RPT. Therefore, we

previously adapted DPM for RPT applications by sampling decay locations internally within the voxelated

geometry.[21] We have previously demonstrated the use of DPM for efficiently performing direct MC

140   dosimetry in patients undergoing ^{131}I radioimmunotherapy,[22,23] radioiodine therapy[24], ^{90}Y

radioembolization[25] and very recently ^{177}Lu-DOTATATE peptide receptor radionuclide therapy[26]. Thus

far, DPM benchmarking for RPT consisted of comparison with estimates from EGS4 and OLINDA.[21,22]

Although some initial measurements with TLDs were performed to experimentally validate the photon

contribution[21], no experimental validation of the beta component of DPM was undertaken at the time,

145   due to the challenges associated with the short range. To our knowledge, prior experimental studies

undertaken by others have also not attempted to directly measure absorbed dose deposition in water

equivalent or high-density mediums by beta emitters that have a range as low as that of the betas

associated with ^{177}Lu.

Motivated by the recent surge in interest in RPT dosimetry and the scarcity of experimental

150   measurements relevant to validating dosimetry calculations in RPT, our goal was to design a practical

and reproducible experimental setup for measuring the absorbed dose deposited in water/tissue by

beta emitting therapy radionuclides. We then use our experimental setup to perform a full (electron +

photon components) validation of our in house DPM MC code for ^{90}Y and ^{177}Lu. Secondary

benchmarking of Monte Carlo N-Particle version 6.2[27] (MCNP6) code as well as the general purpose

155   EGSnrc[28] against the experimental results was also performed, as both are widely available/used for RPT

dosimetry.

2. Materials and Methods

2.1 Experiments

160   Two types of measurements were performed with the RF. The first was a measurement of absorbed

dose to a single sheet of film (SF) and the second was measurement of radionuclide depth dose (DD)

curves using a stack of films. Absorbed doses were measured for ^{177}Lu (in the form of ^{177}Lu DOTATATE)

and ^{90}Y (in the form of ^{90}YCl$_3$) in saline (S) and a bone (B) equivalent solution. Two different thicknesses

of tape (used between the film and the radioactive solution) were tested for ^{177}Lu. The nomenclature

165   used to identify each experiment is indicated in the last column of Table 2.

2.1.1 Phantom Design

The main challenge with experimental measurements that are relevant to RPT dosimetry are the short beta particle ranges and the need to have the radioactive material in liquid form. These considerations were key to our final design of the phantom, which is shown in Figure 1 and Figure 2.

170

The phantom was modeled using computer aided design (CAD) software and 3D printed utilizing a Form 2 printer using stereolithography in a photopolymer resin. Each phantom was designed as a half-cylinder with an open cavity and three top holes used for filling the volume with the radioactive liquid as seen in Figure 1. The phantom cavity size was chosen to provide a smooth absorbed dose distribution across the center 1cm x 1cm area of the film measurement. External dimensions were modeled to fit inside a standard 90mL urine sample container, commonly found at most hospitals, in order to contain inadvertent leakage.

After printing, the model was allowed to dry for 24 hours. All excess support structures were manually removed and the front face of the phantom was sanded with a 400 grit diamond plate to improve tape to surface adhesion. A 3.8cm by 6cm length of Kapton tape[29] was mounted across the front of the phantom to enclose the cavity. These taped phantoms were used as the core component in all validation procedures and allowed for a wide variety of experiments to be performed (**Error! Reference source not found.**) with consistent reproducibility.

Gafchromic EBT3 was cut into 3.8cm x 6.0cm strips using a Full Spectrum Laser Hobby Series 20x12 CO Laser Cutter and a small watermark was cut into the top right corner to provide consistent orientation during post-exposure film scanning. Strips were sandwiched in between two taped half-cylinder phantoms before insertion into the standard specimen container per Figure 2.

2.1.2 Activity Measurement and Solution Preparation

190   The ^{177}Lu and ^{90}Y activities used for the different experiments ranged from 13 - 450 MBq. Injected

activity levels were selected to minimize both exposure during phantom handling and cost, while

providing absorbed dose in the sensitive range for EBT3[9] in each configuration. Prior to each experiment

the necessary exposure time was estimated by scaling the Monte Carlo predicted dose rate for each

geometry by a number of decays until the film absorbed dose was within this sensitive range. This total

195   number of decays was combined with the available radionuclide activity to estimate the required

exposure time. Activities were measured in a Capintec 15R dose calibrator within a 10cc syringe. The

dial setting used was 55 x 10 for ^{90}Y[30] and 48 x 10 for ^{177}Lu. The setting for ^{177}Lu was determined by a dial

setting transfer performed in house to match activity readings for a 10cc syringe and for a Schott vial

with the NIST recommended setting[31] of 449 x 10. The activity solutions were combined in a 60cc syringe

200   with either ~30cc of saline or bone equivalent liquid that included ethylenediaminetetraacetate (EDTA)

to avoid any potential absorption from heavy metal radionuclides into the walls of the container.

    The bone equivalent liquid was prepared by combining deionized water with K_2HPO_4 salt at a

ratio of 100g for salt per 67g water, which results in density and linear attenuation coefficient close to

that of cranial bone.[32] The phosphate-buffered saline mixture was assembled with 1xPBS at 7.3 pH with

205   EDTA added until a concentration of 2.5-µM EDTA[33] was reached. For the bone equivalent solution, the

EDTA salt was mixed directly into the solution until a concentration of 2.5-µM was reached.

2.1.3 Measuring Absorbed Dose to Closest Layer using a Single Film

    A single strip of 3.8cm by 6.0cm Gafchromic EBT3 film was placed between the two phantom

210   halves and then secured in a standard specimen container. A cross sectional view of each material layer

is shown in Figure 2A. Two phantom halves were each enclosed with Kapton tape (12.7 or 25.4µm) and

filled with radioactive solution. The entire center cavity of each phantom half was filled for a total of ~33cc of fluid, ~16.5ml in each half. The semi-clear nature of the 3D print material allowed for visual confirmation of the solution level in each phantom during filling. Precise solution volumes were

215 calculated from calibrated digital scale measurements of the empty, filled, and residual syringes as well as the empty and full phantoms. Phantoms were shielded and secured in locked facilities for 3-47 hours before the film was removed.

220

2.1.4 Measuring Absorbed Depth Dose using Stacked Films

Measurement of radionuclide absorbed depth dose curves was also completed using a very similar phantom setup, except that only one phantom half was used in this case. The single phantom half was

225 enclosed with 25.4μm thick Kapton tape and filled with radioactive solution. The cavity of the single phantom half was filled full, resulting in a total of ~16.5ml of solution. Five (for ^{177}Lu measurements) to ten (for ^{90}Y measurements) 3.8cm by 6.0cm Gafchromic EBT3 films were placed in between the single phantom half and a backscatter stack of water equivalent acrylic and then secured in a standard specimen container.   A cross sectional view of the layers are shown in Figure 2B. Phantoms were

230 shielded and secured in locked facilities for 20-48hrs before the stack of films was removed.

2.2 Film Analysis

Post-exposure optical film scanning was done on an EPSON XL10000 flatbed scanner at 200 dpi with all image correction features turned off. All films were centered in the middle 1/4th of the scanner to avoid

235   lateral response artifacts and a glass compression plate was used to prevent deformation of the film

during scanning.

2.2.1 Calibration Films

Calibration films were created on a Varian TrueBeam Linear Accelerator that was calibrated per TG-51

240   standards[5] using a 6MV photon beam. Ten calibration films were created over a 0-1850cGy range with a

geometric dose sequence at 0, 79.7, 159.5, 319.0, 478.4, 717.7, 877.1, 1116.4, 1594.8, and 1834.0cGy.

Eight additional calibration films were created at the same time as a secondary validation set for

checking the accuracy of the final fits. The average difference between our calibration curve and the

calibration check films in our measured range was 0.1% and the maximum difference for a single film

245   was 2.2%.

The 10 original calibration films were optically scanned and used to fit a continuous calibration curve for

each of the red, blue, and green color channels. Triple-channel dosimetry optimization methods[34] were

250   used to help correct the scanned images for all measurements. The reported absorbed dose values were

computed from the triple-channel optimization reported red channel values.   The calibration fits were

created in FilmQA Pro[35] using their color rational cubic fit shown in equation 1 and Figure 3 where X(D)

is the color channel value, A, B, C, E, and F are the cubic fit parameters, and D is the known delivered

dose.

255

$$X(D) = \frac{(A+BD+CD^2+ED^3)}{(D+F)} \tag{1}$$

2.2.2 Experimental Film Analysis

Film analysis was performed using FilmQA Pro software. Each experimental film was optically scanned

260   with both the measurement film and an unexposed film strip from the same sheet of EBT3 in a single

session. All experimental film measurements were analyzed using a film calibration from the same film

production batch as the experiment. An average over the 1cm x 1cm square at the center of the

exposed film area was used to calculate the mean dose to the film.

Compensation for post exposure film darkening,[36] often accomplished by using the single scan

265   protocol,[37] was instead corrected by closely matching the post-exposure optical scan time between the

calibration strips and the experimental measurements as well as using the dose shift single point

recalibration provided by Ashland.[38] Equation 2 gives the dose shift single point recalibration with X(D)

being the RGB value, D as the original dose, and x and a as scaling factors calculated from the

differences between the experimental scan's unexposed film and the calibration scan's unexposed film.

$$X(D) = x(a + D) \tag{2}$$

270   All ^{90}Y experiments were allowed between 145-176 hours for development while ^{177}Lu films

were measured between 45-100hrs. Calibration curves were rescanned to match the experimental film

development time with no more than a 4% difference in total film development time for the ^{177}Lu and a

maximum 11% development time difference for ^{90}Y.

275   **2.3 Monte Carlo Simulations**

Simulations of the experiments were performed using our in-house DPM program as well as two

general purpose MC codes: MCNP and EGSnrc. A computational phantom for DPM, MCNP, and EGSnrc

was created based on the material and geometry specifications of the 3D printed phantom, the Kapton

tape and manufacturers specifications for Gafchromic film. The material compositions were obtained

280   from Compendium of Material Composition Data for Radiation Transport Modeling[39], and

RADIOCHROMIC FILM: Role and Applications in Radiation Dosimetry[9] and are given in appendix Table

A5. As DPM is designed to perform dose transport on voxelized geometries (for example, patient PET/CT

or SPECT/CT images) the phantom design was voxelized. The voxel size was chosen to be 1.25 x 1.25 x

0.0127mm to model the thin film layers while keeping the total calculation time and memory

285   requirements reasonable. No attempt was made to match the simulation voxel size to the flatbed

scanner pixel dimensions as the average over the $1cm^2$ center of the film was well sampled in both

situations and finer MC binning would significantly increase runtimes. This voxelization caused only

<1.2% difference in the film thickness and <5.2% difference in the Kapton tape thickness (appendix

Tables A2 and A3). The voxelization of the phantom also caused all computational phantom material

290   thicknesses to be somewhere between the average physically measured dimensions and the

manufacturers specified thicknesses, therefore we have high confidence in the final model.

The simulated phantom was specified as filled to 3.5cm high, reaching the bottom of the

insertion holes, with water (Figure 1). This filled water volume in the phantom was used to define the

volume containing the radioactive solution with a uniform activity distribution throughout.

295   The beta energy spectra for all simulations were those generated by BetaShape software version

1.0 available from the Laboratoire National Henri Becquerel.[40] Photon, x-ray, auger electron, and

electron capture spectrums were acquired from NuDat 3.0 via Brookhaven National Laboratory.[41]

Simulations for ^{90}Y included only the beta energy spectrum and no transport was attempted on any x-

ray, auger, or conversion electron portions of ^{90}Y decay due to their minimal contribution to absorbed

300   dose. Simulation for ^{177}Lu did include modeling of x-rays and monoenergetic electrons. No attempt was

made to model absorbed dose contribution from contaminants that may be present in the radionuclide

solution, such as [42] ^{177m}Lu in ^{177}Lu DOTATATE, or ^{90}Sr in ^{90}Y-Cl$_3$[43] depending on the method used to produce the radionuclide.

In the DPM simulations, low energy beta and photon cutoffs were set to 20keV and 4keV

305   respectively and the energy of source betas and/or x-rays born below or reaching the respective cutoffs was deposited locally. To test the validity of this assumption, we started with a much higher beta cutoff (100 keV) and re-ran with lower cutoff values until the difference in absorbed dose-rate values was <0.5%. With the mean free path of ~0.1mm for a 4 keV photon in tissue being less than the minimum distance from the fluid to the active layer of the radiochromic film (~150um) and only ~7% of the total

310   absorbed dose coming from photons, we did not observe meaningful differences when lowering the cutoff under 4 keV. A total of 8 billion decays spread uniformly throughout the solution were simulated, giving an uncertainty of <0.5% in the center 1cm^2 of the first film of each simulation. Run times varied depending on the isotope from 13-90 hours of CPU time on a 2.7GHz Intel Xeon E5-2697v2.

MCNP calculations were defined in the same way as the DPM setup, with a few exceptions.

315   Instead of a uniform voxel distribution the geometry was defined via MCNP's macrobody and universe style definitions. The same beta and photon spectra and electron yields described above for DPM were included for transport in MCNP. Energy cutoffs were matched to the DPM run. MCNP simulations were run for 1 billion histories, due to the much longer run times of a general-purpose MC code, giving an uncertainty of <1.0% in the center of each film. Run times varied depending on the isotope from 880-

320   3690 hours of CPU time on a 3.4GHz AMD Threadripper 1950x. MCNP simulations were run on 16 processors to obtain results in <10 days.

EGSnrc calculations were also defined as close to the DPM setup as possible. Instead of a uniform voxel distribution the geometry was defined via EGSnrc's C++ geometry module.   The same beta and photon spectra and electron yields described above for DPM were included for dose transport

325   in EGSnrc. Energy cutoffs and number of histories were matched to the DPM run. This gave an

uncertainty of <0.5% in the center of each film. Run times varied depending on the isotope from 46-562

hours of CPU time on a 3.4GHz AMD Threadripper 1950x.

3. Results

330

A total of 55 films were analyzed over the course of 20 experiments. The first plot in Figure 4

shows all experimental absorbed dose readings vs the DPM predictions across a wide range of dose

(41.7-1561.6cGy). The central plot in Figure 4 shows experiment vs MCNP calculations for all

experimental configurations and the final plot shows experiment vs EGSnrc.

335   Horizontal and vertical profiles from all MC simulations as well as experimental measurement

from our single film geometry, Figure 5, show the design provides a uniform absorbed dose region

across the center film planes.

3.1 Single Film Results: Dose to Closest Layer

340   The agreement between measurement and each of the three MC estimated absorbed doses are

given in Table 3 for the different single film experiments. The agreement between the absorbed dose

estimates from the RF measurements and DPM was on average -4.0% (range -10.9% to 3.2%) for all

single film ^{177}Lu experiments and was on average -1.0% (range -2.7% to 0.7%) for all single film ^{90}Y.

345

The contribution from the beta emissions to the total absorbed dose deposited in the single films was calculated with MC, which showed that the primary contribution to the absorbed dose was indeed the beta particles for all configurations. Absorbed dose to the Lu177 $_{SF,S,25.4}$ film was 93% from the beta, Lu177 $_{SF,S,12.7}$ was 94% and Lu177 $_{SF,B,25.4}$ was 90%. The conversion electrons and auger electrons

350   contributed <0.15% of dose to the first layer of the film. The rest of the contribution (7 to 10%) in the ^{177}Lu experiments is from photons (x-rays and gamma-rays), which are dominated by the emissions at 113 keV and 208 keV.[41] Dose from ^{90}Y experiments was considered to be effectively 100% from the betas as no other starting particles were simulated due to their negligible dose contributions. All dose from secondary particles, i.e. Bremsstrahlung, was grouped as part of the starting particle dose estimate

355   in the MC simulation tallies.

3.2 Stacked Film Results: Depth Dose

The agreement between measurement and DPM, EGSnrc, and MCNP estimated absorbed doses are

360   given in

as well as Figures 6 and 7 for the different stacked film experiments. Depth dose estimates by DPM agreed with RF measurement on average 1.2% (range -8.0% to 15.2%) across all depths for ^{177}Lu and on average 4.0% (range -5.0% to 9.3%) across all depths for [90]Y. At the deepest measured depth (1.3152mm) the ^{177}Lu film measurement received only 5.9% of the absorbed dose that the shallowest

365   film (0.2032mm) received.

MC simulations predicted that absorbed dose from betas was 92.8%, 63.5%, 13.2%, 1.6% and 1.2% of the total (betas + others) going from the film closest to the ^{177}Lu solution to the furthest as seen in Figure 8, indicating a large component of the beta dose was measured across our design.

370

The measured absorbed doses for ^{90}Y showed closer agreement to the MC code estimates than the ^{177}Lu across all 10 depths. Absorbed dose to the 10th film (2.7052mm) was 11.4% of the dose to the shallowest (0.2032mm). Due to the longer range of the ^{90}Y beta complete measurement across the

375 entire beta range was not attempted with this phantom geometry.

MC calculations done using EGSnrc, MCNP, and DPM agreed with each other across the board, within 4.7% and within 3.4% for ^{177}Lu and ^{90}Y respectively, for all geometries and across all depths.

3.3 Uncertainty Estimation

Overall uncertainty in the measurement was determined by evaluating the level of

380 reproducibility across repeated experiments. Table 2 shows each of the 7 experimental setups along with the number of times each experiment was attempted, with 2-4 repetitions for any given configuration. The coefficient of variation of the absorbed dose rate across all the runs of each setup was between 0.0-4.5% for the[177]Lu experiments and 1.0-6.0% for the Y-90 experiments. The coefficient of variation for single films was 0.5-3.0% (Table 3) and for the depth dose measurements 0.0–6.0%

385 (Table 4).

Although individual components contributing to the uncertainty in the recorded dose-rates are difficult to measure and uncertainty propagation challenging, some estimates can be made. Use of the Capintec 15R dose calibrator for each of the radionuclide activity measurements provides a high degree

of accuracy.   Zimmerman et. al.[30] gives ~1-2% uncertainty for a [90]Y Capintec 15R measurement using a

390   10ml syringe and Denis E. Bergeron and Jeffrey T. Cessna[31] estimate their dose calibration uncertainty at

~1%. The geometry dependence of the dose calibrator reading was also verified to have a minimal

impact on our activity measurement (Figure A2) and a sensitivity analysis was completed to estimate

potential error in activity measurement across both dose calibrators and dial settings (**Error! Reference**

source not found.A1). The uncertainty in the phantom fluid-volume measurement that also contributes

395   to the uncertainty in the activity is expected to be negligible based on the scale validation data given in

Figure A1.

Variability in experimental geometry for any given experiment was evaluated by repeated

caliper measurements of the 3D printed phantom, Kapton tape, and RF. Agreement between the 3D

print and the CAD design was within ~3% (Table A4), except for wall thickness, which is not expected to

400   impact the overall dose-rate measurement. Variation in Kapton film thickness was 4 – 5% (Table A3) and

RF layer thicknesses was ~1% (Table A2).

Among factors associated with RF measurement/calibration uncertainty are calibration curve

fitting, and post-exposure film darkening. The uncertainty associated with film calibration curve fitting is

estimated as 0.1% on average and up to 2.2 % for any given film (Section 2.2.2). Variations in post-

405   exposure film darkening were evaluated across multiple post-exposure timepoints from 1-400 hours for

a subset of the experiments. Both calibration films and experimental films were rescanned at 8 post-

exposure timepoints and dose to the central 1cm^2 was measured to quantify the variation in only using a

single recalibration film strip. This rescanning protocol also evaluates overall film analysis repeatability

by including variation in flatbed scanner light/heat levels, film position on the scanner, among other

410   things. A standard deviation of 4.4% was found across the varied post-exposure readout film subset,

giving us high confidence in the repeatability of the film analysis procedures.

Statistical uncertainties associated with the MC simulations were well under 0.5% according to the estimates provided by all three MC codes, with the shorter 1 billion history MCNP runs having the highest uncertainties. Potential uncertainty in the simulations due to parameters such as photon or

415   electron cutoffs, step size, and the voxelization sizes are expected to be larger contributions than statistical uncertainty and are estimated at ~0.5% (Section 2.3)

4 Discussion

Experimental validation of the absorbed dose estimation step is critical for clinical translation of

420   dosimetry guided RPTs. This is however, rarely undertaken due to the challenges of measuring dose deposited in tissue by short range particles such as the betas associated with ^{177}Lu. In this study we design, construct, and test a simple phantom for RF-film based measurement of beta and gamma components of ^{177}Lu and ^{90}Y absorbed doses, which is then used to validate our in-house developed DPM MC dosimetry code. The single film geometry provided for a wide variety of experiments to be

425   performed, allowing for several aspects of the setup to be tested independently without substantial increases in time or experimental complexity. Variations on the transport medium, either saline or bone equivalent fluid, and depth to the film, via Kapton tape thickness, were easily implemented. Further changes to the 3D printed cavity height, depth, or shape for any given radionuclide have not been evaluated yet, but the platform we have developed will allow such evaluation in the future. The depth

430   dose measurements showed the high level of agreement between DPM and experiment in regions both dominated by beta energy deposition and by photon deposition. Figure 6B and Figure 7B show the relative differences between DPM, MCNP, and EGSnrc vs the experiment. When the DPM vs experiment difference increases, the MCNP vs experiment difference and EGSnrc experiment difference also increase, and vice versa. While the magnitude of the difference for each comparison varies, the overall

435   trends match across all three MC simulations.

Dose to film for both measured radionuclides showed excellent agreement with DPM regardless of experimental setup, with an average of -4.0% for all single film ^{177}Lu experiments, 1.2% for depth dose ^{177}Lu, -1.0% for single film ^{90}Y, and 4.0% for depth dose [90]Y (Table 3,4). The average difference between measurement and simulation was within the overall measurement uncertainty estimated from the

440   repeats. While four of the five single film experimental geometries showed an average agreement of <2% with DPM, the bone liquid experiment (Lu177 $_{SF,B,25.4}$) was an outlier with a 10.2% difference between measurement and simulation. With both MCNP and EGSnrc also showing relatively large discrepancies compared with experiment, 6.8% and 8.2% respectively, experimental setup variation associated with the challenges of working with the bone liquid is likely the primary factor for this

445   disagreement. Additional investigation using FilmQA Pro revealed larger non-uniformities in the vertical and horizontal film profiles than was seen in other experimental setups. Mixing of the thick bone solution with the ^{177}Lu DOTATATE may have been insufficient during the filling procedure, potentially creating non-uniform distributions within the phantom volume. We did not see mixing issues with the ^{90}Y chloride in bone solution, however the chloride's yellow tint helped verify the solution was uniformly

450   mixed, whereas the DOTATATE was translucent.

When validating Monte Carlo codes, multiple factors such as step size, cut-off energies, material/geometry specifications can contribute to the difference between experiment and simulation. While specifications for the composition of the phantom material, RF and the Kapton tape were available [32,9], the composition of the silicone adhesive on the tape was not provided by the vendor and

455   was estimated using the entry for silicone. However, the impact of the adhesive material composition appears to be minimal, because the percent difference between absorbed dose-rates from experiment and simulation were very similar when using a much thinner tape/adhesive combination in the ^{177}Lu experiments (Table A3). Additionally, micrometer measurements of multiple film sheets and measurements within any given sheet of RF shows close manufacturing tolerances within the film itself,

460   measuring within 3µm of specification for the film base, active layer, and total thickness (Table A2).

Similar evaluation of the 3D printed phantoms also provided good agreement in every batch of 3D prints

(Table A4).

The radiochromic film energy dependence between the 6MV calibration energy and the

much lower energy betas of ^{177}Lu and ^{90}Y is expected to be minimal as the electron restricted stopping

465   power ratios between EBT3 and water over the 10keV-10MeV range show minimal variation.[44] A 6MV

photon beam was chosen due to the extensive validation of absorbed dose delivery, and because such

beams should be readily available at other institutions. Other photon energies may be used for

calibration[8], however use of low energy photon sources (<50 keV) may need alternative procedures or

calibration factors. The dose rate dependence for EBT3 is minimal,[9] and prior studies with beta-emitting

470   eye plaques have successfully irradiated RF to 30 Gy over 1 week[45], which is ~18 cGy/h compared to the

~1-100 cGy/h used in our study.

The use of relatively low activity radionuclide sources resulted in long exposure times (3-48hrs)

for the validation measurements in our study. A portion of the polymerization process that would

typically be considered "post-exposure" is now taking place alongside the experimental polymerization

475   as the absorbed dose slowly builds up over a course of days. As the post-exposure polymerization can

be approximated by logarithmic fits,[36] the majority of the additional development happens in the first

24-48 hours. In addition, the rate of change in net optical density is dependent on the initial deposited

dose, with higher doses having significantly higher rates of post-exposure polymerization.   This makes

matching calibration curve post-exposure time development to experimental post-exposure time

480   development in RPT applications more complicated than in traditional EBRT film studies. We have

chosen to extend our calibration and experimental scan times to help compensate for any initial changes

in optical densities, but this is an issue that may need further investigation in the future.

Prior work on experimental measurement of short-range beta emitters has shown the viability of using RF as an effective measurement tool for these radionuclides, but lacks the capability to reliably

485   measure at short distances, where a large portion of the dose is deposited for many radionuclides of

interest. Tiwari et al.[11] was able to measure beta energy deposition above 1mm and Villarreal-Barajas

et. al.[14] showed the potential to measure at 0.104mm, but found damage to their first three layers of RF,

and recorded their first clean measurement at 0.416mm. It is unclear if the geometry proposed by

Villarreal-Barajas et al would be reliable at 0.416mm or at any lower distances as only a single

490   measurement appears to have been attempted. The 3D printed phantom developed for this study has

shown the ability to both place the RF within 0.1651mm cleanly and repeatedly.

Future refinements for the phantom would include optimizing the cavity shape/volume for

different radionuclides and for depth dose measurements would include using less sensitive film

(EBTXD) closer to the source and more sensitive (EBT3) further away. Our work could also be extended

495   to other radionuclides not evaluated in the current study including alpha particle emitters. With thinner

Kapton tape and delaminated RF, one can measure the absorbed dose from particles with ranges below

100 microns.

5 Conclusion

The experimental measurements presented in this work validates both electron and photon

500   components of our in-house DPM internal dosimetry code, which we had previously only performed for

photons using TLDs. Furthermore, the experimental setup we present can be used in other clinics for

validating their internal dosimetry calculations/software. Despite the extensive checks and verifications

completed while performing the absorbed dose measurements the overall process is straightforward

and able to be completed in any hospital that has access to RF dosimetry equipment. The level of

505   repeatable results using this relatively simple inexpensive design across experiments was encouraging

for future endeavors. The 20 experiments performed in this setup showed that the combination of 3D printing and film measurement can provide a viable base for inexpensive repeatable measurements that could be used for one time validation or continued (annual) quality assurance in almost any clinic. For short range radionuclide that have increased sensitivity to any variation in experimental setup we were

510   able to obtain measurements with low standard deviations.

Validation of DPM showed remarkably good agreement with experimental measurement, for both single and depth dose geometries, between experiment and DPM, with an average difference of <4%. Experiments that did show higher variation from the DPM calculated values also showed high deviation with the two other MC codes, indicating DPM's transport methodology was likely not the

515   source of disagreement. With the consistent repeatability of experimental setup and measurement, the low level of differences between DPM, MCNP, and EGSnrc, and the high level of agreement between MC and experiment, DPM has shown itself to be a reliable dose transport engine for photons and short/medium range betas relevant to RPT.

Disclosures

530   The authors have no conflicts to disclose.

References

1. Malcolm J, Falzone N, Lee B, Vallis K. Targeted radionuclide therapy: New advances for improvement of patient management and response. *Cancers*. 2019;11(2):268. doi:10.3390/cancers11020268

535   2. St. James S, Bednarz B, Benedict S, et al. Current status of radiopharmaceutical therapy. *International Journal of Radiation Oncology*Biology*Physics*. 2021;109(4):891-901. doi:10.1016/j.ijrobp.2020.08.035

3. Yu EY, Laidley D, Pouliot F, et al. A multicenter, randomized, controlled phase II study: Efficacy and safety of PSMA-targeted Radioligand Therapy I-131-1095 (1095) plus

540   enzalutamide (ENZA) in 18F-DCFPYL PSMA scan avid, metastatic castration-resistant prostate cancer (mcrpc) patients post-abiraterone (ABI) progression (arrow). *Journal of Clinical Oncology*. 2020;38(6_suppl). doi:10.1200/jco.2020.38.6_suppl.tps260

4. Stabin MG, Sharkey RM, Siegel JA. Radar commentary: Evolution and current status of dosimetry in nuclear medicine. *Journal of Nuclear Medicine*. 2011;52(7):1156-1161.

545   doi:10.2967/jnumed.111.088666

5. Almond PR, Biggs PJ, Coursey BM, et al. AAPM's TG-51 protocol for clinical reference dosimetry of high-energy photon and electron beams. *Medical Physics*. 1999;26(9):1847-1870. doi:10.1118/1.598691

6. Rivard MJ, Coursey BM, DeWerd LA, et al. Update of AAPM Task Group No. 43 report: A

550   revised AAPM protocol for brachytherapy dose calculations. *Medical Physics*. 2004;31(3):633-674. doi:10.1118/1.1646040

7. Massillon-JL G, Minniti R, Mitch MG, Maryanski MJ, Soares CG. The use of gel dosimetry to measure the 3D dose distribution of A90SR/90y intravascular brachytherapy seed. *Physics in Medicine and Biology*. 2009;54(6):1661-1672. doi:10.1088/0031-9155/54/6/017

555   8. Niroomand-Rad A, Chiu-Tsao ST, Grams MP, et al. Report of AAPM Task Group 235 radiochromic film dosimetry: An update to TG-55. *Medical Physics*. 2020;47(12):5986-6025. doi:10.1002/mp.14497

9. Das IJ. *Radiochromic Film: Role and Applications in Radiation Dosimetry*. Boca Raton, FL: CRC Press, Taylor & Francis Group; 2018.

560   10. Sgouros G, Bolch WE, Chiti A, et al. ICRU report 96, dosimetry-guided radiopharmaceutical therapy. *Journal of the ICRU*. 2022;21(1):1-212. doi:10.1177/14736691211060117

11. Tiwari A, Sunderland J, Graves SA, Strand S, Flynn R. Absorbed dose distributions from Beta-decaying radionuclides: Experimental validation of Monte Carlo Tools for radiopharmaceutical dosimetry. *Medical Physics*. 2020;47(11):5779-5790.

565   doi:10.1002/mp.14463

12. Jan S, Santin G, Strul D, et al. Gate: A simulation toolkit for PET and SPECT. *Physics in Medicine and Biology*. 2004;49(19):4543-4561. doi:10.1088/0031-9155/49/19/007

13. Kassis AI. Therapeutic radionuclides: Biophysical and Radiobiologic Principles. *Seminars in Nuclear Medicine*. 2008;38(5):358-366. doi:10.1053/j.semnuclmed.2008.05.002

14. E. Villarreal-Barajas J, Ferro-Flores G, Hernandez-Oviedo O. Experimental validation of Monte Carlo depth-dose calculations using radiochromic dye film dosimetry for a beta-gamma 153SM radionuclide applied to the treatment of rheumatoid arthritis. *Radiation Protection Dosimetry*. 2002;101(1):439-444. doi:10.1093/oxfordjournals.rpd.a006021

15. Zaidi H. *Monte Carlo Calculations in Nuclear Medicine*. Second ed. IOP Publishing; 2022.

16. Bolch WE, Bouchet LG, Robertson JS, et al. MIRD pamphlet No. 17: the dosimetry of nonuniform activity distributions--radionuclide S values at the voxel level. Medical Internal Radiation Dose Committee. *J Nucl Med*. 1999;40(1):11S-36S.

17. Tiwari A, Gravesa SA, Sunderland J. The impact of tissue type and density on dose point kernels for patient-specific voxel-wise dosimetry: A Monte Carlo Investigation. *Radiation Research*. 2020;193(6):531. doi:10.1667/rr15563.1

18. Sempau J, Wilderman SJ, Bielajew AF. DPM, a fast, accurate Monte Carlo code optimized for photon and electron radiotherapy treatment planning dose calculations. *Physics in Medicine and Biology*. 2000;45(8):2263-2291. doi:10.1088/0031-9155/45/8/315

19. Chetty IJ, Moran JM, McShan DL, Fraass BA, Wilderman SJ, Bielajew AF. Benchmarking of the dose planning method (DPM) Monte Carlo code using electron beams from a racetrack microtron. *Medical Physics*. 2002;29(6):1035-1041. doi:10.1118/1.1481512

20. Chetty IJ, Moran JM, Nurushev TS, et al. Experimental validation of the DPM Monte Carlo code using minimally scattered electron beams in heterogeneous media. *Physics in Medicine and Biology*. 2002;47(11):1837-1851. doi:10.1088/0031-9155/47/11/301

21. Wilderman SJ, Dewaraja YK. Method for fast CT/SPECT-based 3D Monte Carlo absorbed dose computations in internal emitter therapy. *IEEE Transactions on Nuclear Science*. 2007;54(1):146-151. doi:10.1109/tns.2006.889164

22. Dewaraja YK, Wilderman SJ, Ljungberg M, Koral KF, Zasandy K, Kaminiski MS. Accurate dosimetry in 131I radionuclide therapy using patient-specific, 3-dimensional methods for SPECT reconstruction and absorbed dose calculation. J Nucl Med. 2005 May;46(5):840-9.

23. Dewaraja YK, Schipper MJ, Shen J, et al. Tumor-absorbed dose predicts progression-free survival following 131I-tositumomab radioimmunotherapy. *Journal of Nuclear Medicine*. 2014;55(7):1047-1053. doi:10.2967/jnumed.113.136044

24. Sisson JC, Dewaraja YK, Wizauer EJ, Giordano TJ, Avram AM. Thyroid carcinoma metastasis to skull with infringement of brain: Treatment with Radioiodine. *Thyroid*. 2009;19(3):297-303. doi:10.1089/thy.2008.0426

25. Dewaraja YK, Devasia T, Kaza RK, et al. Prediction of tumor control in 90Y radioembolization by logit models with PET/CT-based dose metrics. *Journal of Nuclear Medicine*. 2019;61(1):104-111. doi:10.2967/jnumed.119.226472

26. Dewaraja YK, Mirando DM, Peterson A, et al. A pipeline for automated voxel dosimetry: Application in patients with multi-SPECT/CT imaging following 177lu peptide receptor radionuclide therapy. *Journal of Nuclear Medicine*. April 2022. doi:10.2967/jnumed.121.263738

27. Goorley T, James M, Booth T, et al. Initial MCNP6 release Overview. *Nuclear Technology*. 2012;180(3):298-315. doi:10.13182/nt11-135

28. Kawrakow I, Rogers D, Mainegra-Hing E, Tessier F, Townson R, and Walters B. EGSnrc toolkit for Monte Carlo simulation of ionizing radiation transport, doi:10.4224/40001303 [release v2021], 2000.

29. DuPont Kapton HN polyimide film datasheet. Dupont.com. https://www.dupont.com/content/dam/dupont/amer/us/en/products/ei-transformation/documents/DEC-Kapton-HN-datasheet.pdf. Accessed May 25, 2021.

30. Zimmerman BE, Cessna JT, Millican MA. Experimental determination of calibration settings for plastic syringes containing solutions of 90Y using commercial radionuclide calibrators. *Applied Radiation and Isotopes*. 2004;60(2-4):511-517. doi:10.1016/j.apradiso.2003.11.068

31. Bergeron DE, Cessna JT. An update on 'dose calibrator' settings for nuclides used in nuclear medicine. *Nuclear Medicine Communications*. 2018;39(6):500-504. doi:10.1097/mnm.0000000000000833

32. de Dreuille O, Strijckmans V, Ameida P, Loc'h C, Bendriem B. Bone equivalent liquid solution to assess accuracy of transmission measurements in SPECT and Pet. *IEEE Transactions on Nuclear Science*. 1997;44(3):1186-1190. doi:10.1109/23.596985

33. Park M-A, Mahmood A, Zimmerman RE, Limpa-Amara N, Makrigiorgos GM, Moore SC. Adsorption of metallic radionuclides on Plastic Phantom walls. *Medical Physics*. 2008;35(4):1606-1610. doi:10.1118/1.2871191

34. Micke A, Lewis DF, Yu X. Multichannel Film Dosimetry with nonuniformity correction. *Medical Physics*. 2011;38(5):2523-2534. doi:10.1118/1.3576105

35. Film QA Pro. *FilmQA Pro Users Guide*. www.gafchromic.com/filmqa-software/filmqapro/. Accessed July 16, 2021.

36. Palmer AL, Bradley D, Nisbet A. Evaluation and implementation of triple-channel Radiochromic Film Dosimetry in Brachytherapy. *Journal of Applied Clinical Medical Physics*. 2014;15(4):280-296. doi:10.1120/jacmp.v15i4.4854

37. Lewis D, Micke A, Yu X, Chan MF. An efficient protocol for radiochromic film dosimetry combining calibration and measurement in a single scan. *Medical Physics*. 2012;39(10):6339-6350. doi:10.1118/1.4754797

38. Micke A. Gafchromic protocol. GafChromic Protocol Workshops Europe February 2015. http://www.gafchromic.com/documents/Micke_GafChromic_Protocol_Europe_201502%20C.pdf. Accessed January 18, 2022.

39. Detwiler R, McConn R, Grimes T, Upton S, Engel E. Compendium of material composition data for Radiation Transport Modeling. 2021. doi:10.2172/1782721

40. Mougeot X. Erratum: Reliability of usual assumptions in the calculation OFBANDNSPECTRA [phys. rev. C91, 055504 (2015)]. *Physical Review C*. 2015;92(5). doi:10.1103/physrevc.92.059902

41. National Nuclear Data Center NuDat (Nuclear Structure and Decay Data). NuDat 3. https://www.nndc.bnl.gov/nudat3/. Accessed December 18, 2021.

42. Kock AL. STC-18-042-licensing of lutetium-177. LICENSING OF LUTETIUM-177 (STC-18-042) (2018). https://www.nrc.gov/docs/ML1815/ML18156A589.pdf. Accessed August 6, 2021.

43. Wike JS, Guyer CE, Ramey DW, Phillips BP. Chemistry for commercial scale production of yttrium-90 for Medical Research. *International Journal of Radiation Applications and Instrumentation Part A Applied Radiation and Isotopes*. 1990;41(9):861-865. doi:10.1016/0883-2889(90)90064-n

44. Sutherland JG, Rogers DW. Monte Carlo calculated absorbed-dose energy dependence of EBT and EBT2 film. *Medical Physics*. 2010;37(3):1110-1116. doi:10.1118/1.3301574

45. Trichter S, Soares CG, Zaider M, DeWyngaert JK, DeWerd LA, Kleiman NJ. 15 years of 106 Ru Eye plaque dosimetry at Memorial Sloan-Kettering Cancer Center and Weill Cornell Medical Center using radiochromic film in a solid water phantom. *Biomedical Physics & Engineering Express*. 2018;4(4):045017. doi:10.1088/2057-1976/aab674

670   **Appendix**

A. Verification of Experimental Parameters

When using experimental measurement to validate MC simulation, it is imperative that physical

properties such as material composition, material thicknesses, and injected activities used in the MC

model be highly accurate. For this work we carefully verified these parameters as shown below.

675   **A. 1. Activity Verification**

        Activity measurements used in this study were taken using a Capintec 15R dose calibrator. For

Y-90, the Capintec 15R activity measurements were checked against two other dose calibrators in our

pharmacy. A sensitivity analysis was completed to estimate potential error in activity measurement

across both dose calibrators and dial settings **Error! Reference source not found.**A1. All activity

680   measurements were taken in a 10cc syringe placed in the center of the dose calibrator holder

A. 2. Activity/Experimental Process Verification

        The phantom radionuclide activity was calculated based on the weight of the saline injected into

the phantom. These injections ranged between 30-35ml per experiment and was measured on an

685   available digital scale. We performed a calibration for the scale which is shown in Figure A1. Calibration

was completed across the 1-50g range and no major deviations were seen over the measured range.

The syringe used for activity injection into each phantom was also checked to make sure the dose

calibrator activity in the syringe was consistent over the entire range of 0-10ml for ^{177}Lu. Figure A2

690   shows the dose calibrator reading from <0.5ml to >9.5ml and which has good linearity over the whole

range, so no additional calibration curve was applied to the dose calibrator readings.

A. 3. Physical Model Dimension Verification

695   Both Gafchromic EBT3 film and Kapton tape thickness measurements were acquired using a

Mitutoyo 293-344-30 micrometer. Three sets of measurements were taken at different points across 3

reference film cutouts to measure the total thickness and then the film was carefully peeled apart and

each layer was measured individually. Results showed an active layer thickness of 25.1 µm and a base

thickness of 128µm, very close to the values used in our simulation models, 25.4µm and 127µm

700   respectively. These results are presented in Table A2.

Kapton tape thickness was measured at 5 locations across multiple strips of tape and averaged

values are reported in Table A3. The tape is composed of two materials, a layer of Kapton film and a

layer of silicone adhesive. Two tape thicknesses were used in our experiments: a 25.4µm thick Kapton

tape with a 38.1µm thick adhesive layer, and a 12.7µm thick Kapton tape with a 12.7µm thick adhesive

705   layer. Manual verification of the overall thickness of each tape strip showed close agreement with the

manufacturer's listed thicknesses with ~4-5% difference.

The 3D printed phantom was also measured using the same micrometer to verify printing

tolerances. Three different phantoms were randomly selected, and four sections of the phantom were

710   measured; the thickness of the top, the radial width, the thickness of the bottom and the side wall

thickness. Table A4 shows the results with only the sidewall thickness showing a substantial deviation

from the modeled values. This may be due to the interaction between the curvature of the wall and the

micrometer's flat sensor face. It is not expected that the wall thickness will substantially affect the

results in any way for this experimental design as the overall change in volume is negligible and any

715   displaced fluid is not in near proximity to the film measurement.

A. 4. Simulation Material Compositions

Material compositions and densities for each simulation have been included in this appendix for

future reference and/or result reproducibility.

720

725

755

Figure Legend Listing – For typesetting use only

Figure 1: 3D CAD cross-sectional and photo views of a phantom half-cylinder (A) alongside entire assembly views of the taped and filled finished product with exploded CAD model (B). Three filling ports with corks for sealing (red objects in (A and B)) were used to facilitate the filling process and reduce back pressure.

760

Figure 2: Cross-sectional view of each material layer at the center of the single film phantom to measure absorbed dose-to-closest-layer phantom (A) and stacked film phantom to measure absorbed depth dose (B). In B, 5 and 10 film layers were used for ^{177}Lu and ^{90}Y, respectively.

765   *Figure 3: Rational cubic film calibration curve 150hrs after initial exposure.*

Figure 4: Complete experimental absorbed dose comparisons across all doses, measurements, and computation engines. Identity line shown in black.

Figure 5: Vertical and horizontal linear profiles for both evaluated radionuclides. Profiles were obtained from single film experimental geometries with a saline medium. Scanned images of representative exposed films are inset under each horizontal profile.

Figure 6: Depth dose curves for both ^{177}Lu depth dose experiments showing (A) absolute absorbed dose values (B) percentage differences relative to experiment

770

Figure 7: Depth dose curves for three ^{90}Y depth dose experiments showing (A) absolute absorbed dose values and (B)

percentage differences relative to experiment

775   *Figure 8: Absorbed dose contribution from beta and gamma. Values calculated in DPM for the Lu177$_{DD,S,25.4}$ experimental geometry*
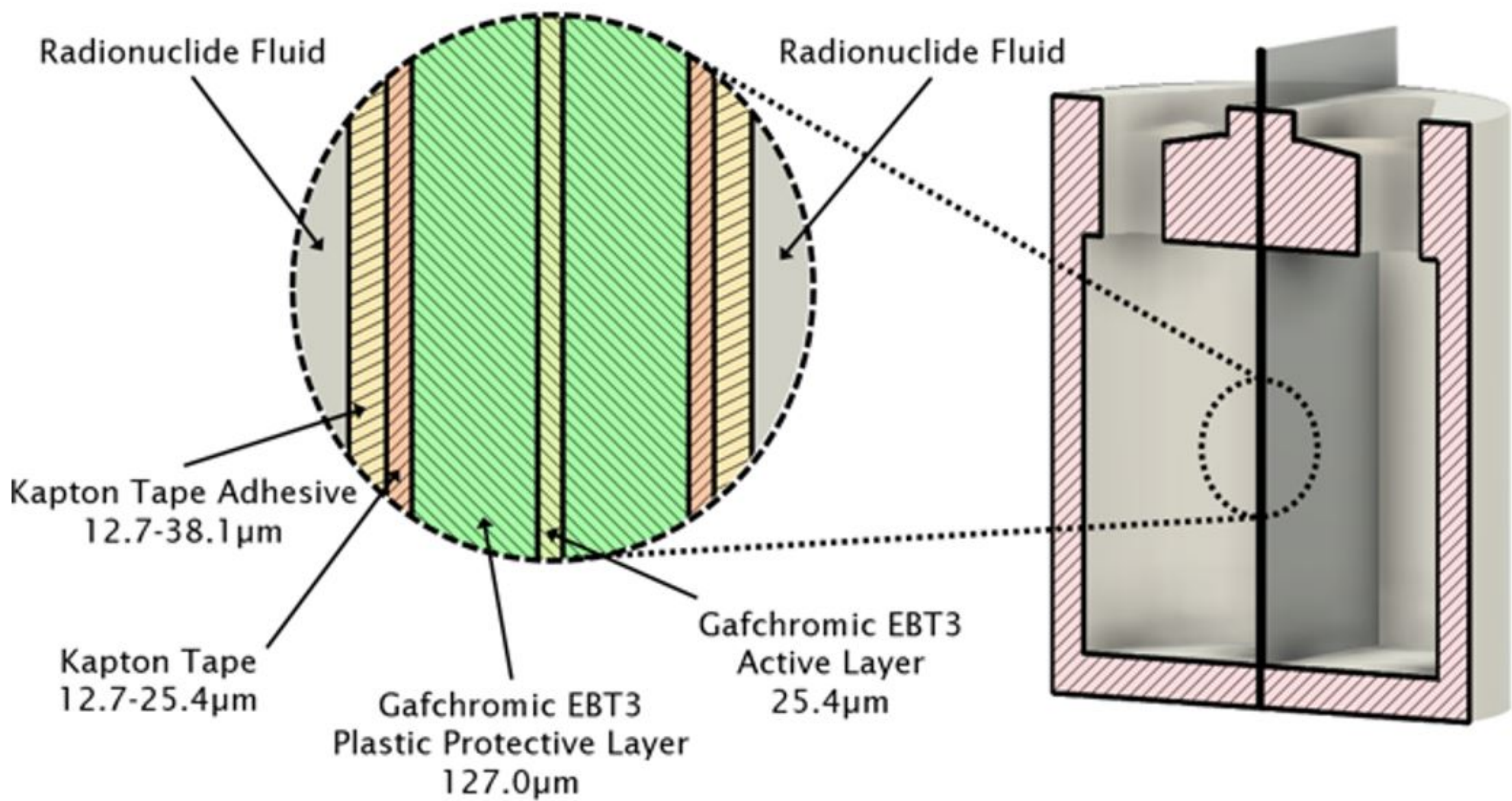

Figure A1: Measurement of scale linearity from 1 to 50g using calibrated weights.

Figure A2: Variation in dose calibrator readout for ^{177}Lu 10cc syringe. Linear response across entire range of radionuclide fill level within syringe.
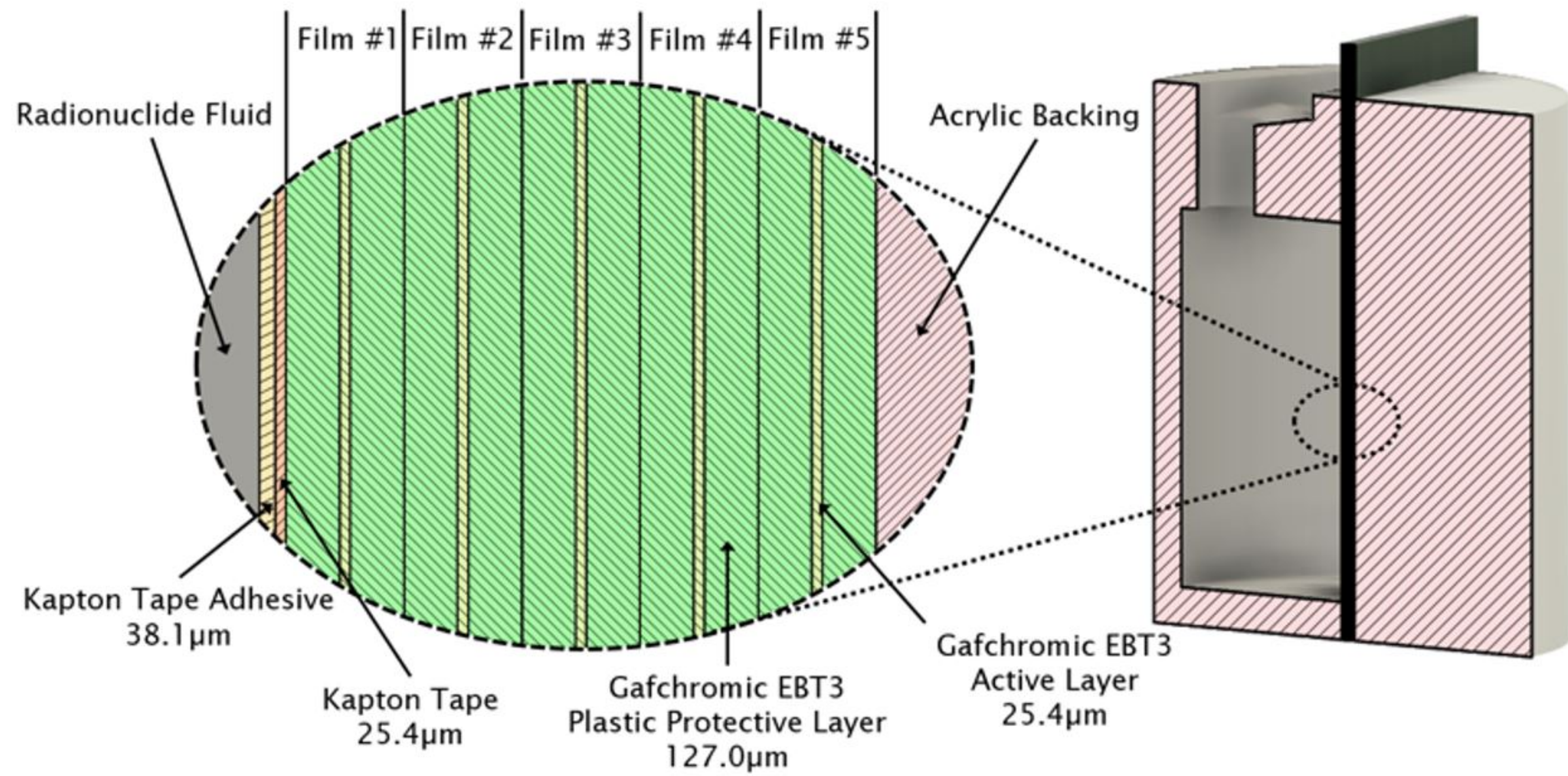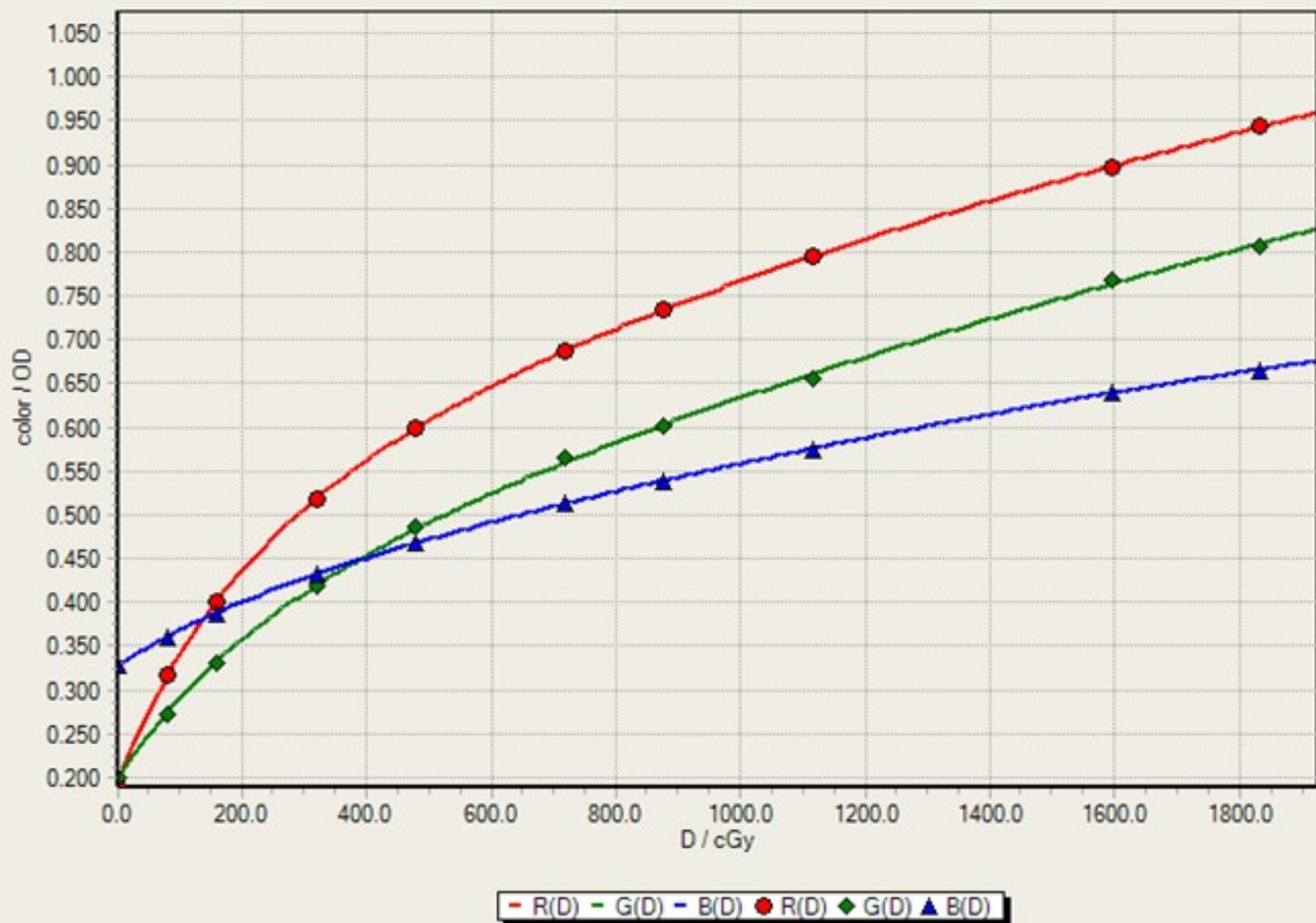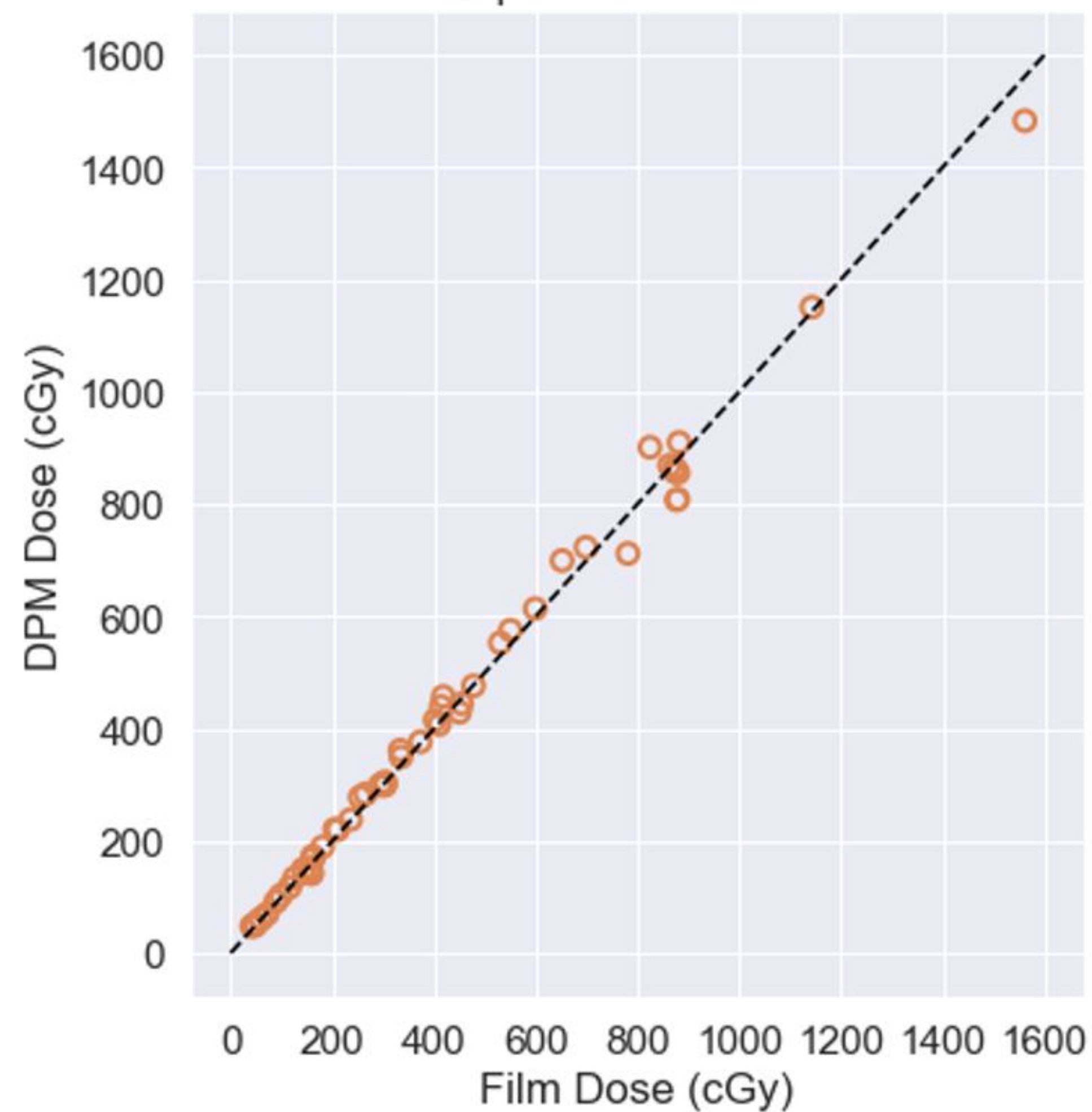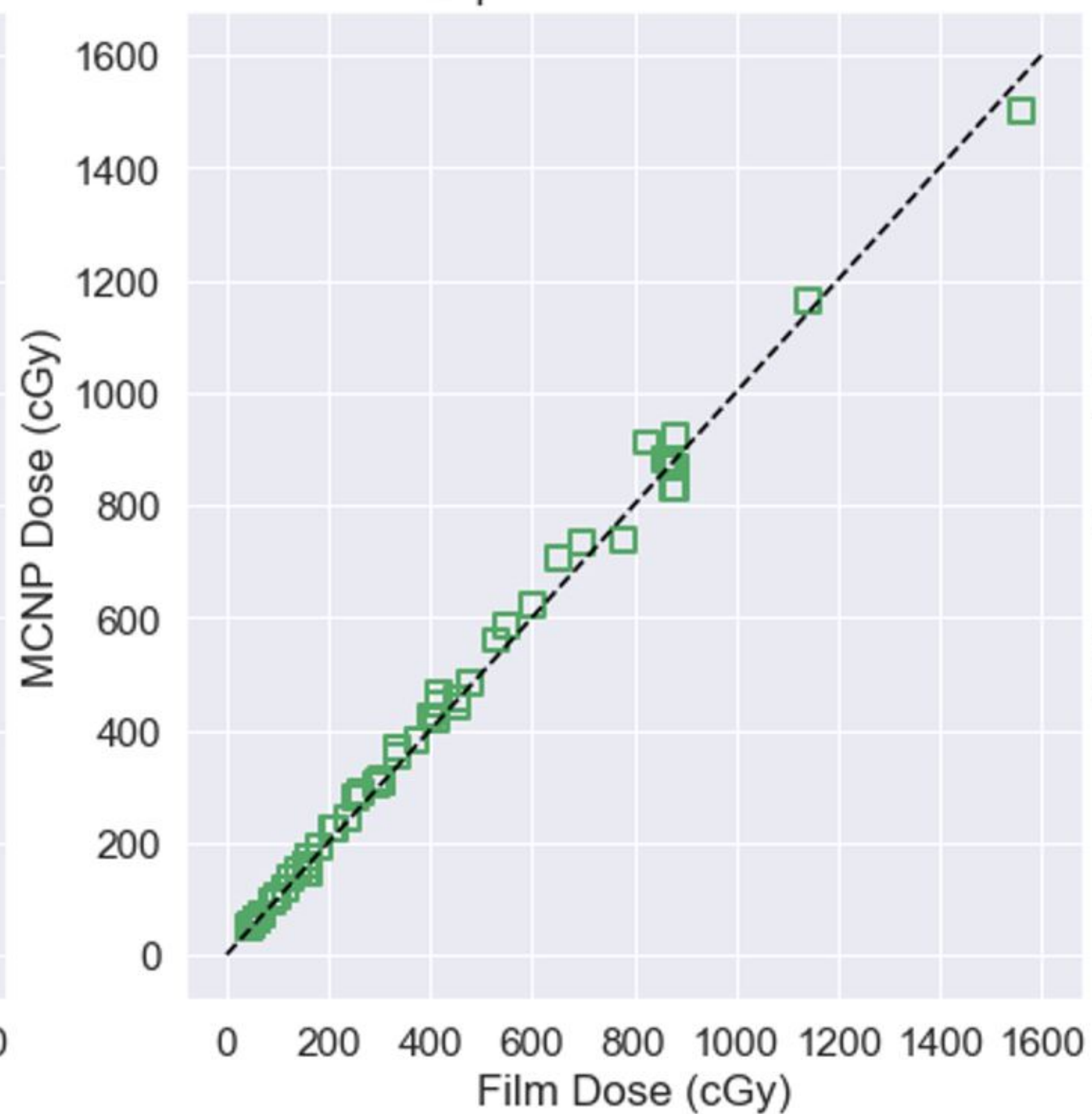
780

A Single Film

Radionuclide Fluid

Radionuclide Fluid

Kapton Tape Adhesive
12.7-38.1μm

Kapton Tape
12.7-25.4μm

Gafchromic EBT3
Plastic Protective Layer
127.0μm

Gafchromic EBT3
Active Layer
25.4μm

B Depth Dose

Film #1 | Film #2 | Film #3 | Film #4 | Film #5

Radionuclide Fluid

Acrylic Backing

Kapton Tape Adhesive
38.1μm

Kapton Tape
25.4μm

Gafchromic EBT3
Plastic Protective Layer
127.0μm

Gafchromic EBT3
Active Layer
25.4μm

Absorbed Dose Measurements

Absorbed Dose Linear Profile Curves
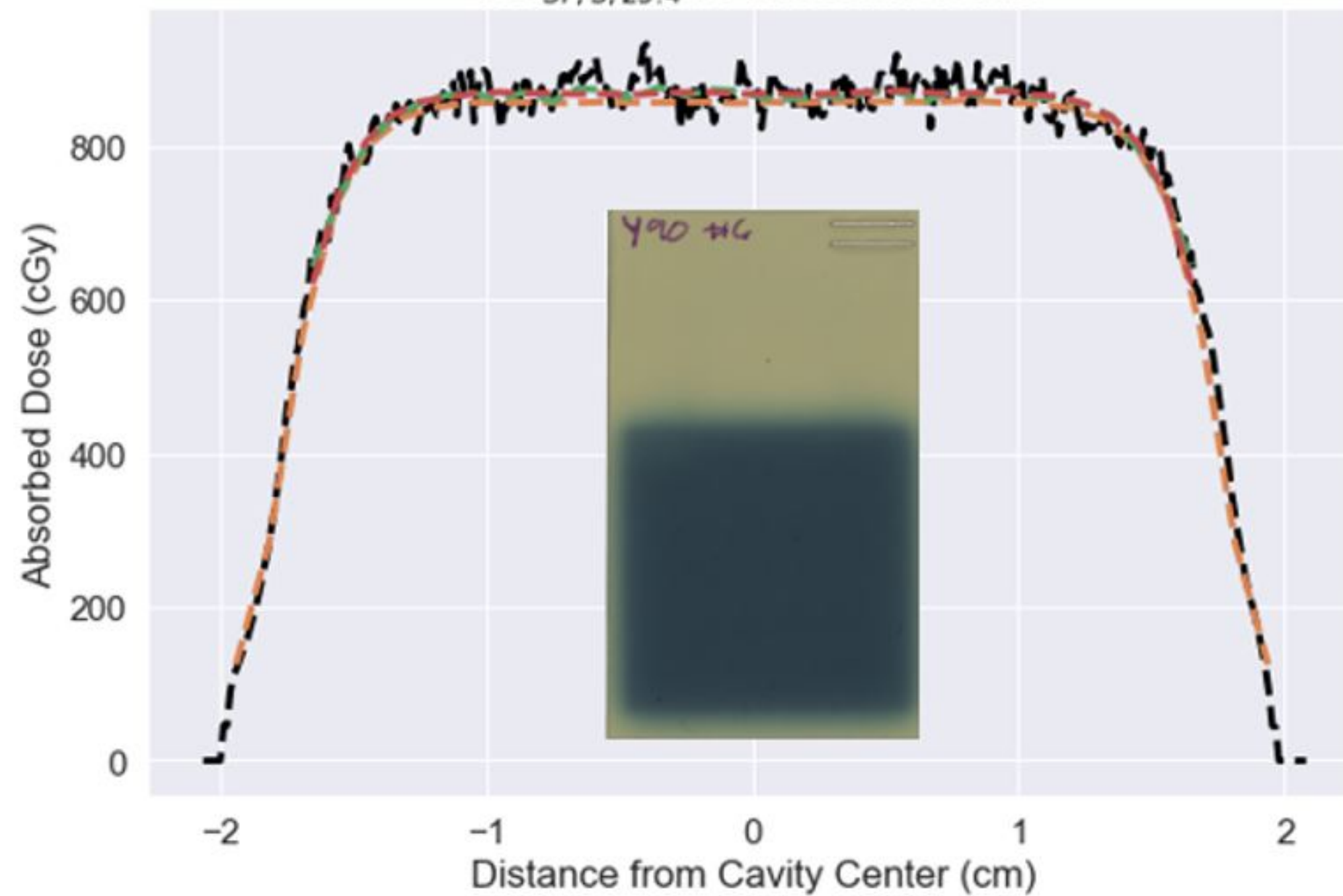

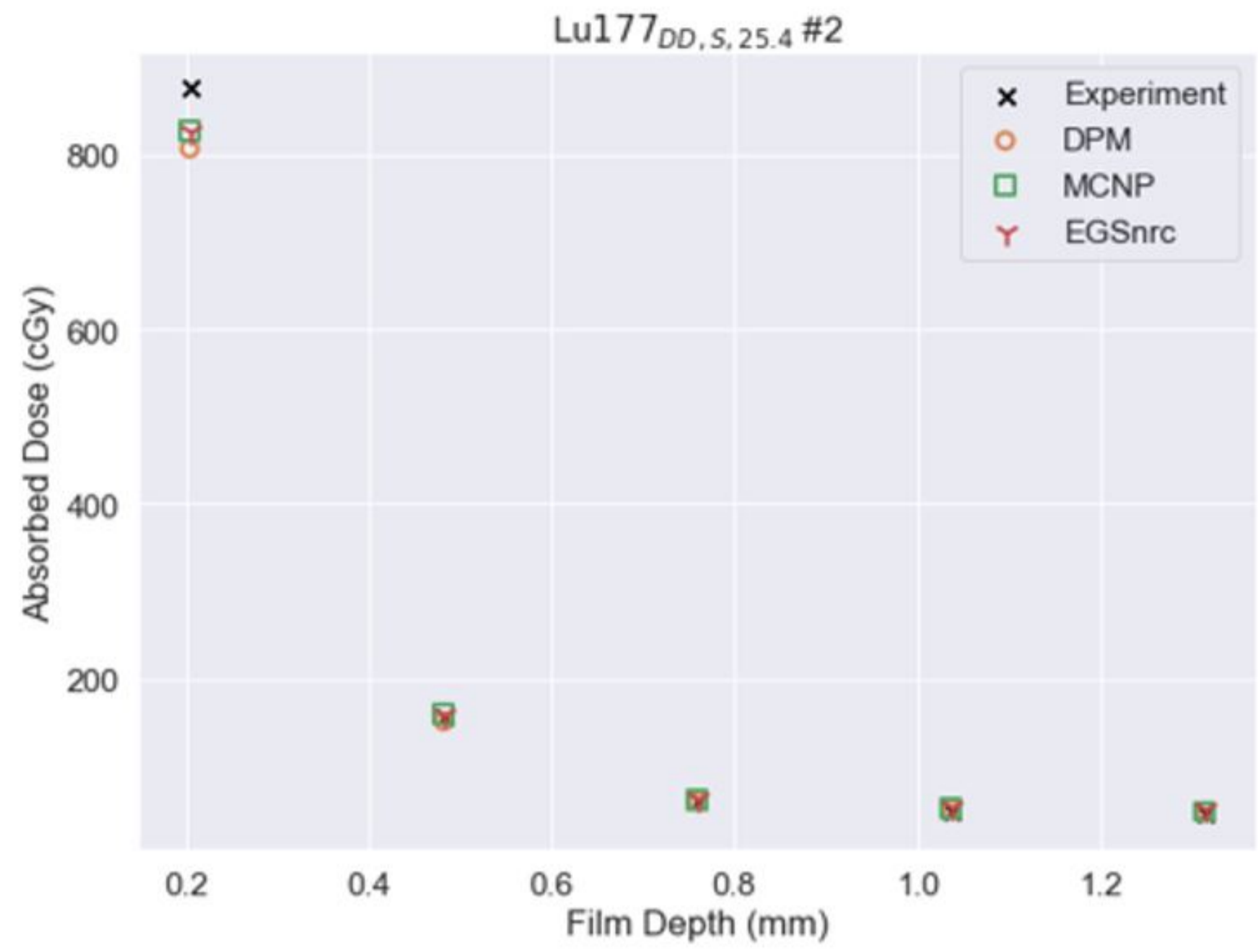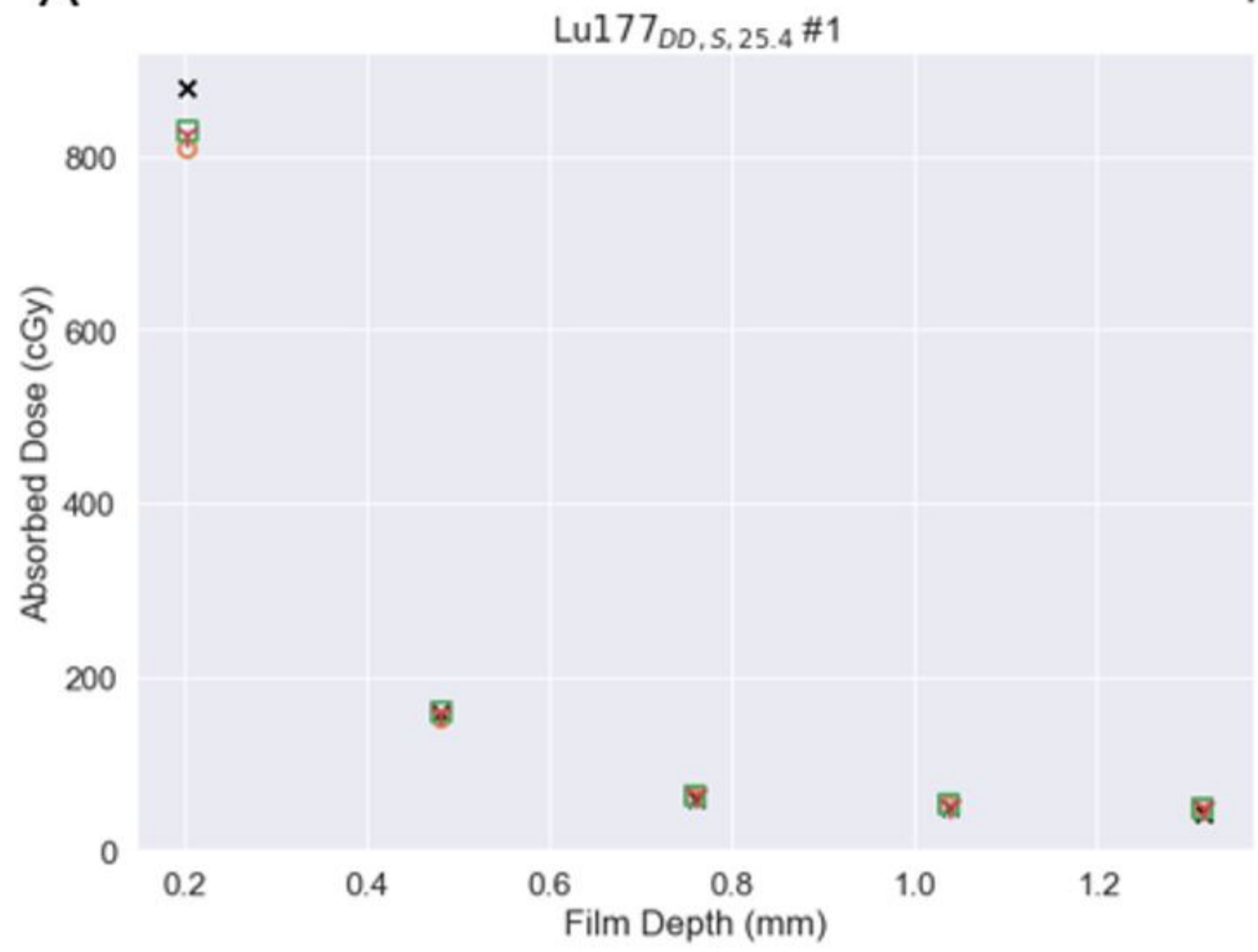Lu177$_{SF,S,25.4}$ #3 Vertical Profile
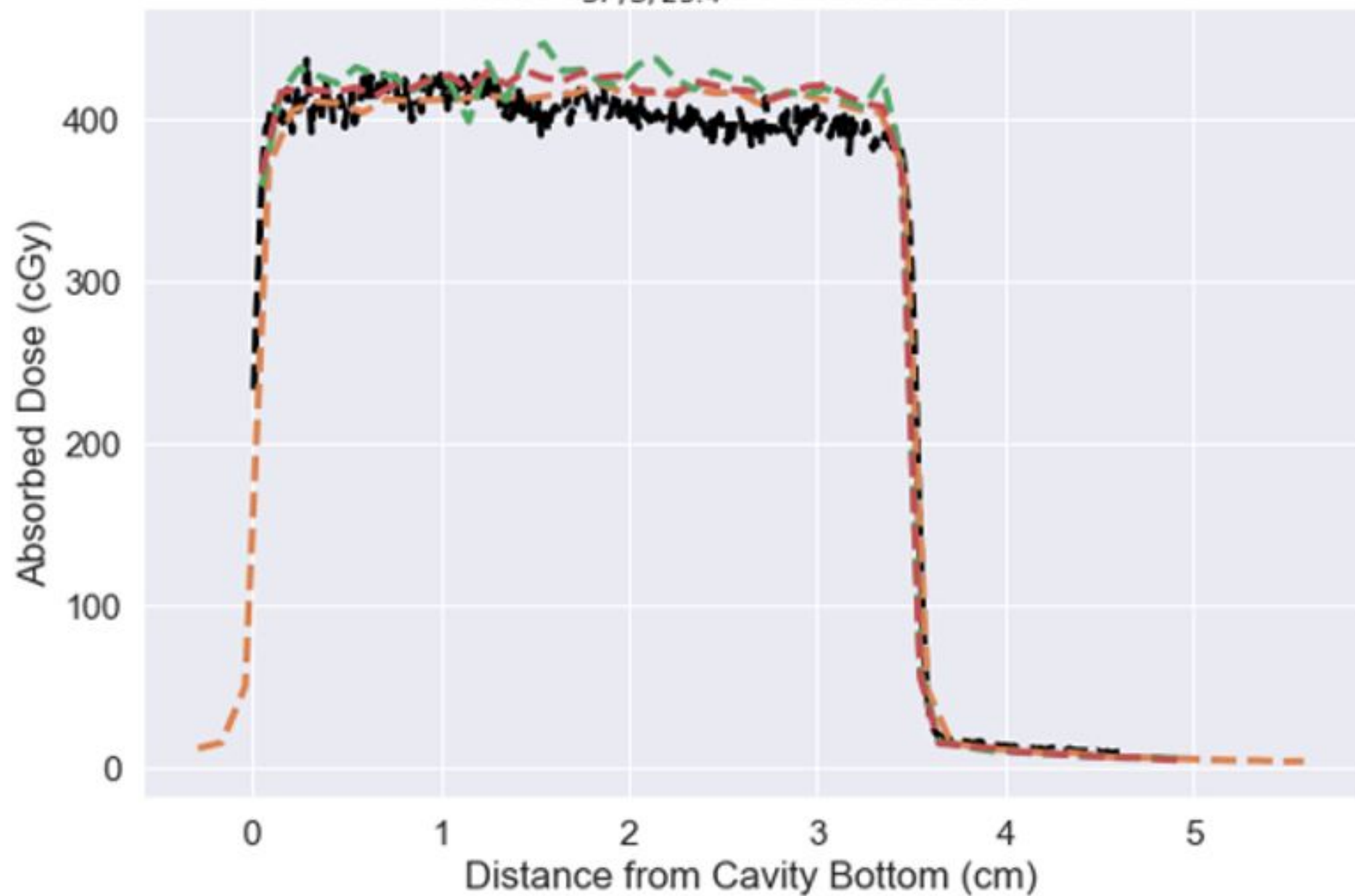
Y90$_{SF,S,25.4}$ #3 Vertical Profile
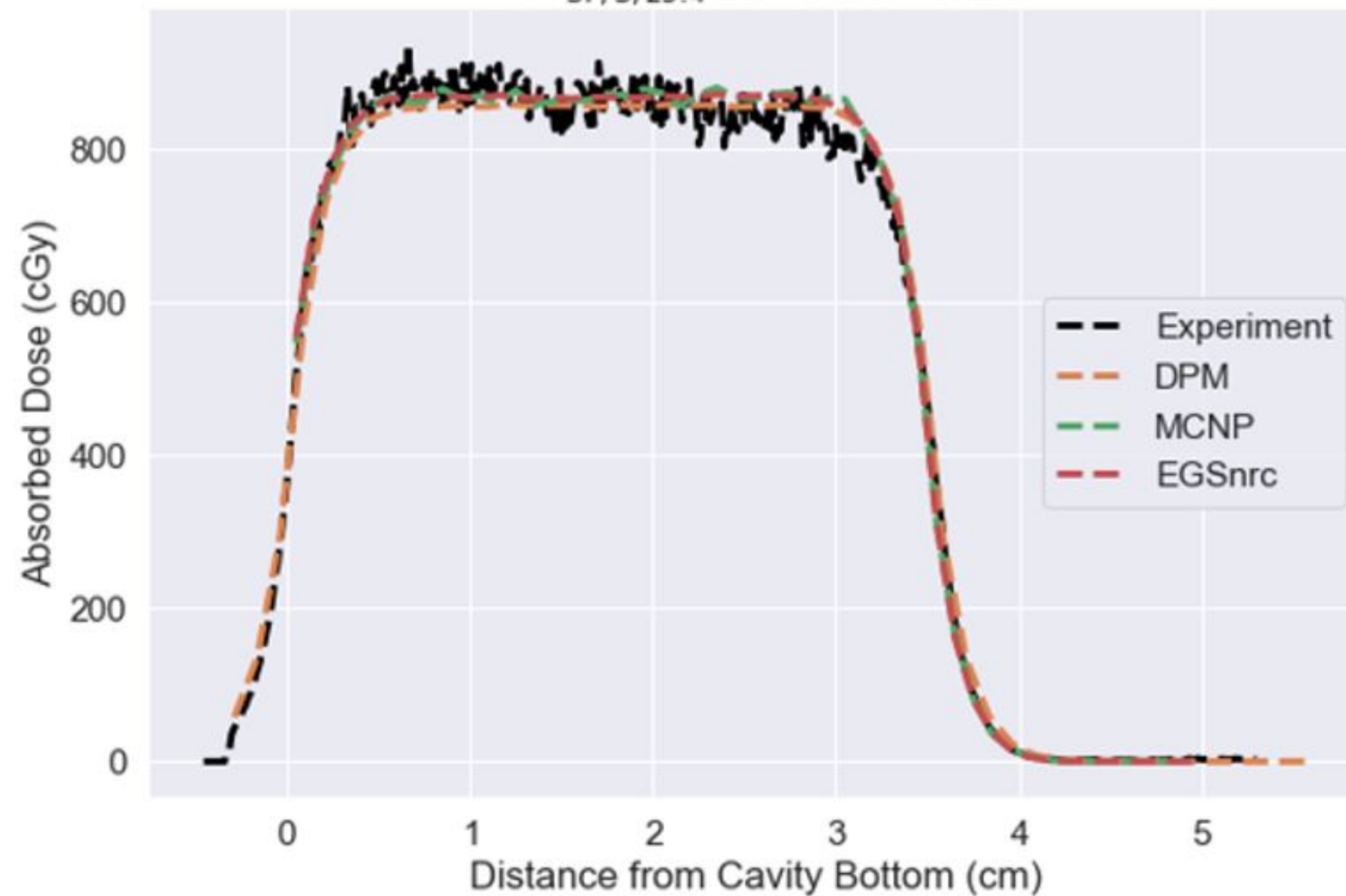
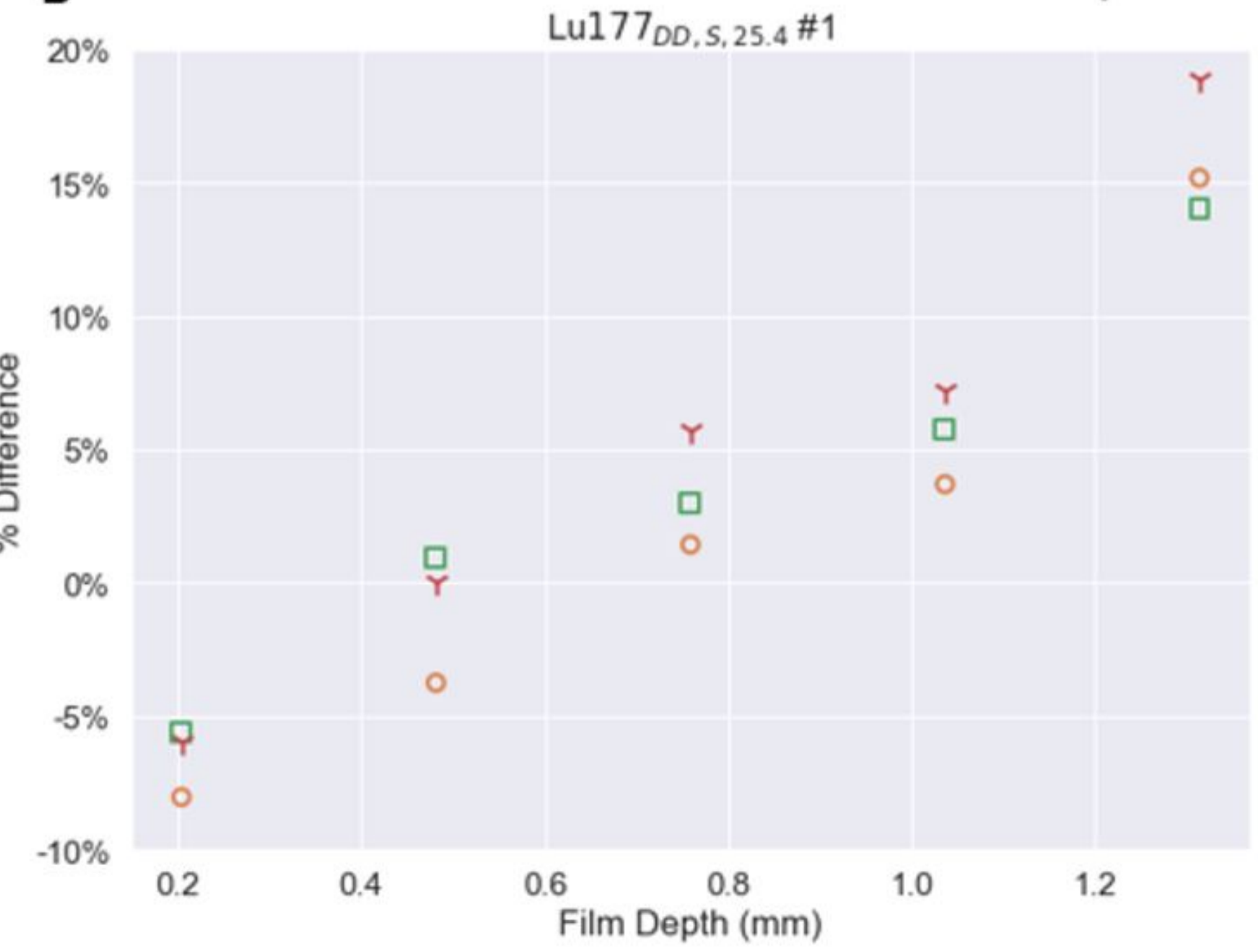Lu177$_{SF,S,25.4}$ #3 Horizontal Profile
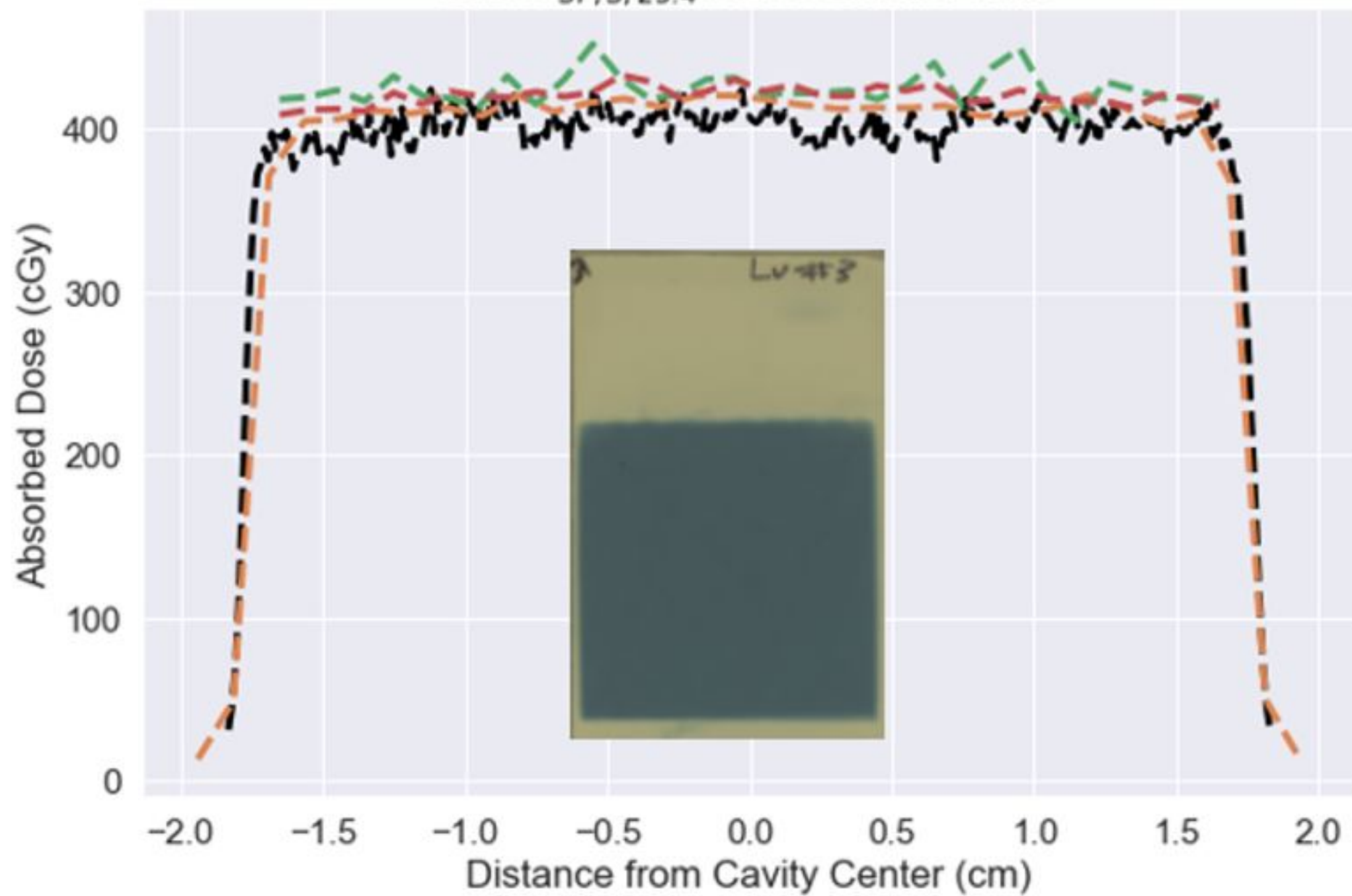
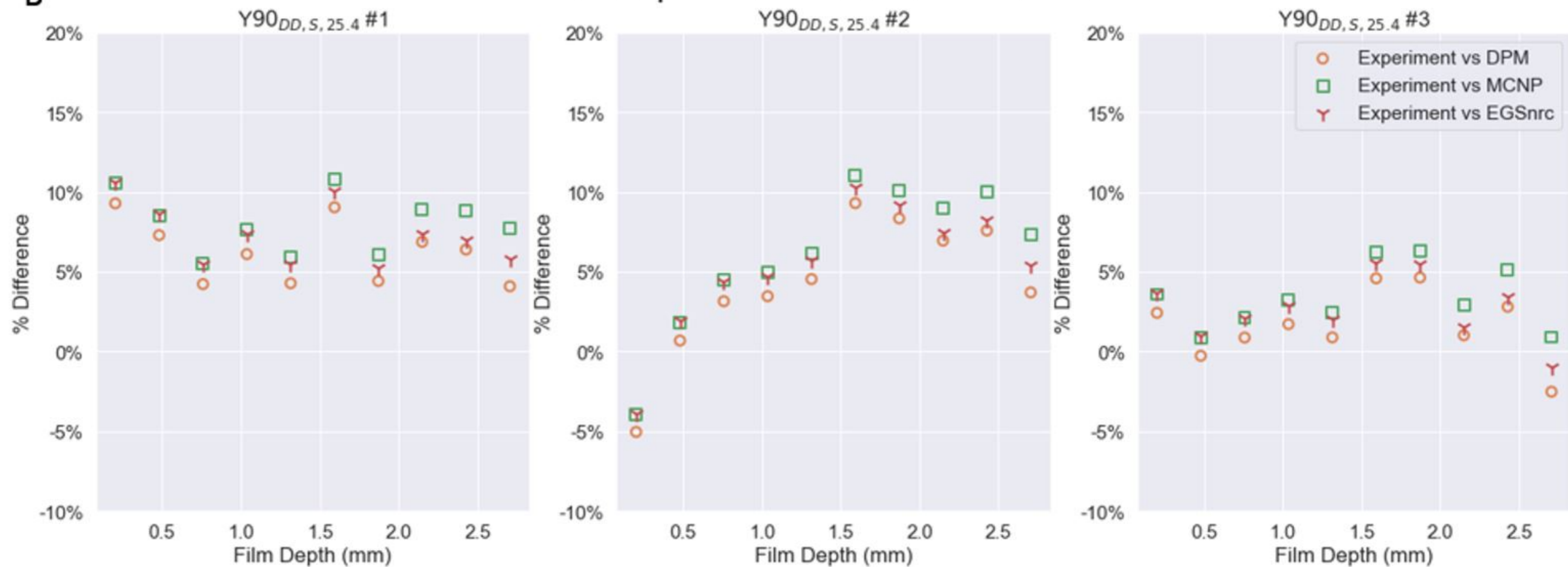Y90$_{SF,S,25.4}$ #3 Horizontal Profile

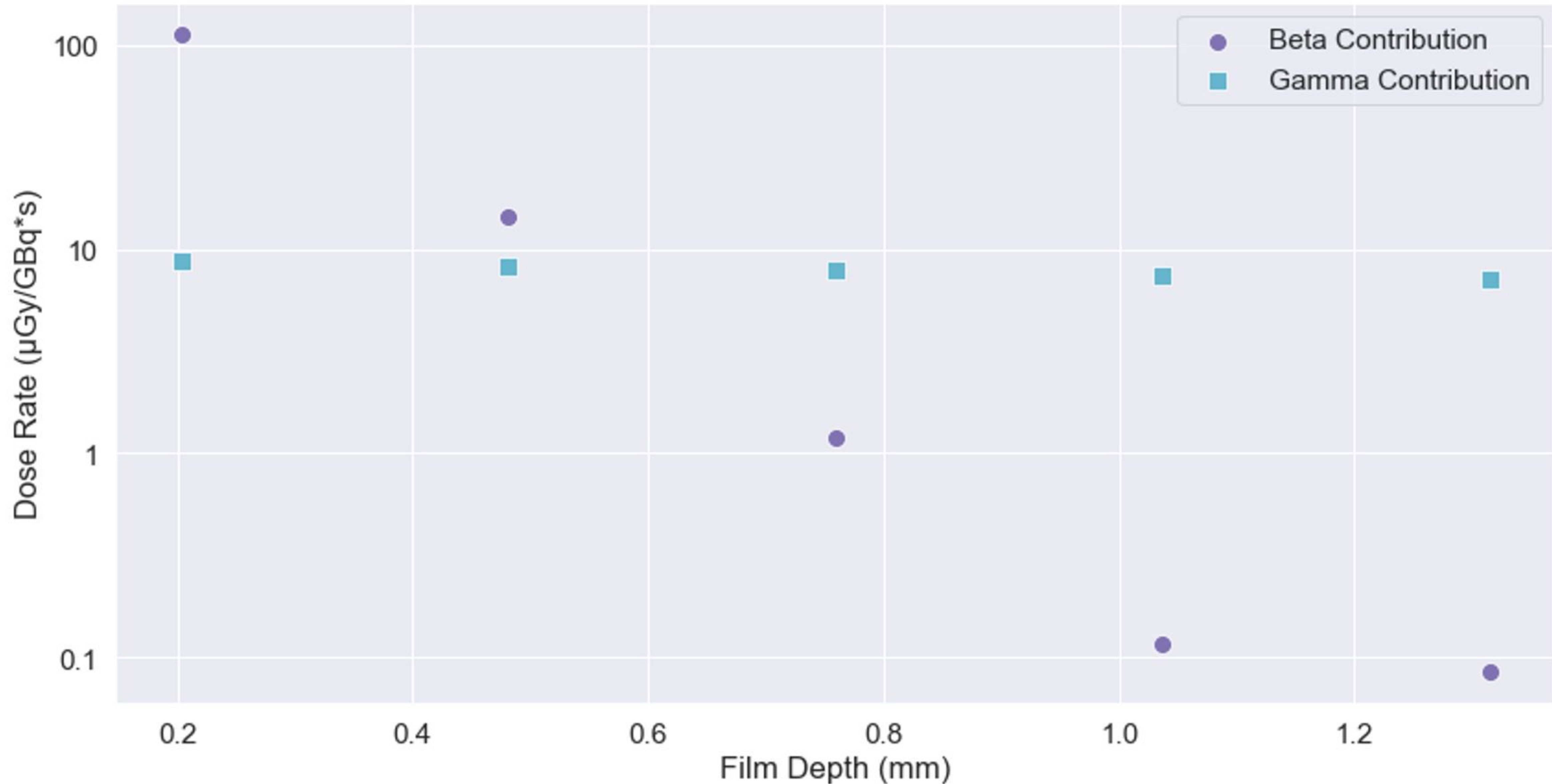Figure A. Y-90 Depth Dose Curves

Figure B. Y-90 Depth Dose Curve Differences

Lu-177 Absorbed Dose Rate Contribution by Emitted Particle Type

Scale Verification
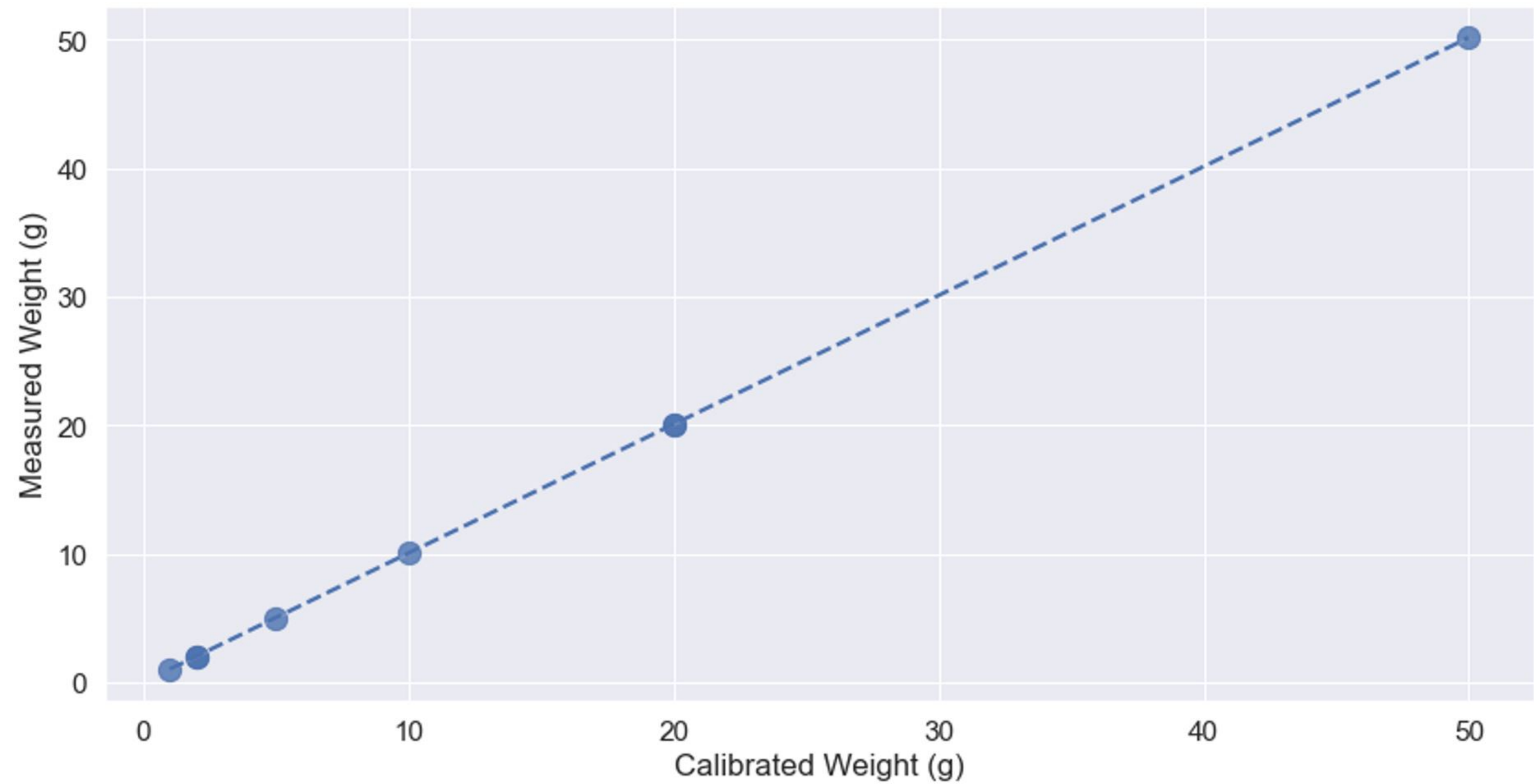
Lu-177 Weight vs Activity
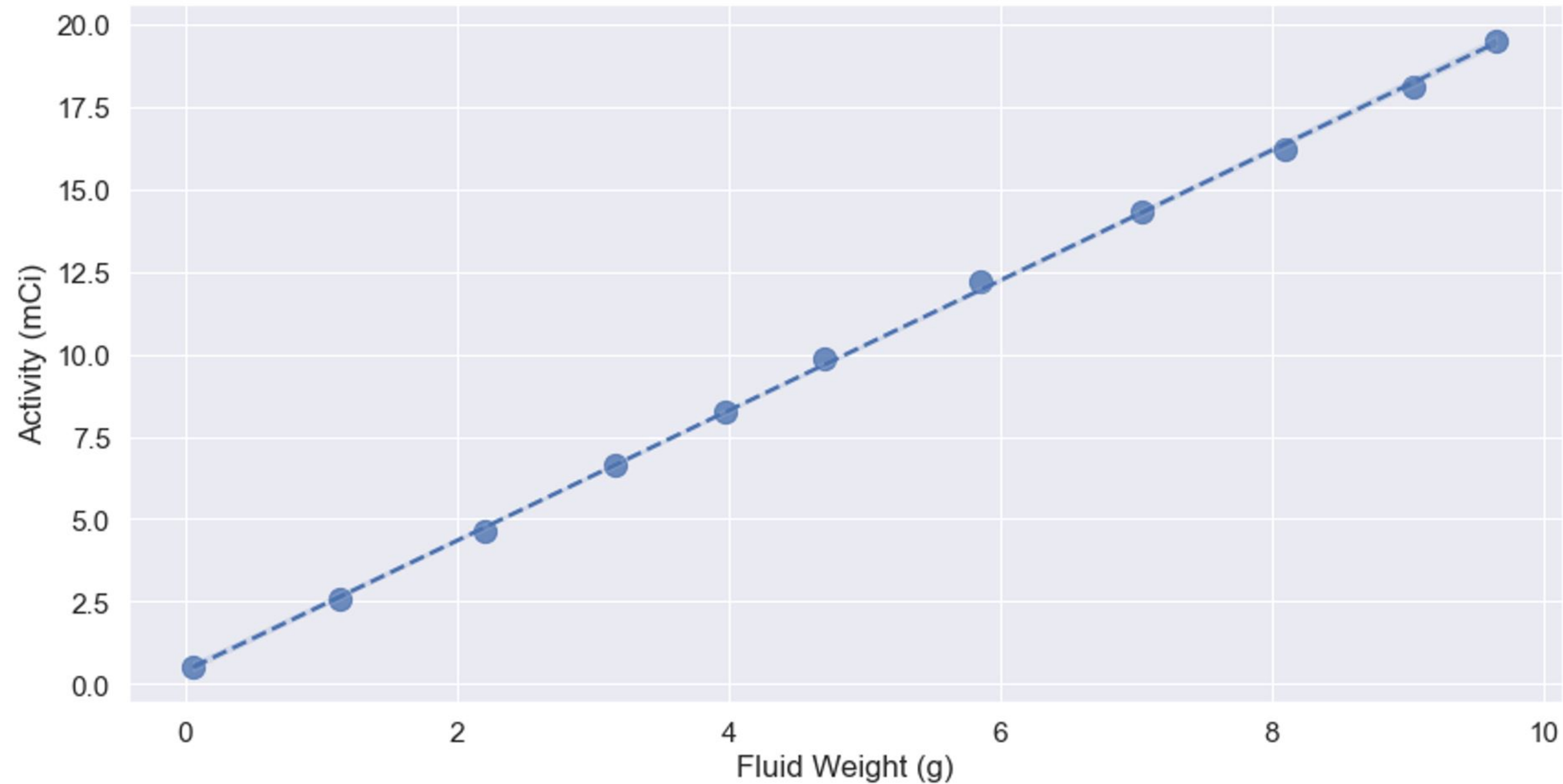
Table 1: Beta emitters of interest in RPT and their physical characteristics[10]

Nuclide	Half-life	Mean Beta Energy (keV)	Maximum Beta Energy (keV)	CSDA range for maximum beta energy (mm)
^{177}Lu	6.71 d	133	497	1.8
^{124}I	4.18 d	188	610	2.3
^{131}I	8.02 d	182	606	2.3
^{153}Sm	46.3 h	225	705	2.8
^{186}Re	3.72 d	323	1070	4.4
^{89}Sr	50.5 d	583	1490	7.1
^{188}Re	17.0 h	765	2120	10
^{90}Y	2.67 d	934	2280	11

Note: Continuous slowing down approximation (CSDA) range is an approximation of the average distance traveled by a charged particle. The displayed CSDA range only includes the range of the highest energy beta for the radionuclide.

Table 1: Variations in experimental setup parameters

Radionuclide*	Measurement Type	Liquid Solution	Measurement Depth (mm)	Kapton** Tape Thickness	Repeat Measurements	Experimental Setup Name
^{177}Lu	Single Film	Saline	0.2032	25.4μm	4	Lu177$_{SF,S,25.4}$
	Single Film	Saline	0.1651	12.7μm	2	Lu177$_{SF,S,12.7}$
	Single Film	Liquid bone	0.2032	25.4μm	3	Lu177$_{SF,B,25.4}$
	Depth dose	Saline	0.2032–1.3152	25.4μm	2	Lu177$_{DD,S,25.4}$
^{90}Y	Single film	Saline	0.2032	25.4μm	4	Y90 $_{SF,S,25.4}$
	Single Film	Liquid bone	0.2032	25.4μm	2	Y90 $_{SF,B,25.4}$
	Depth dose	Saline	0.2032-2.7052	25.4μm	3	Y90 $_{DD,S,25.4}$

*^{177}Lu DOTATATE [Novartis], ^{90}Y Chloride [Eckert & Ziegler]

**Used to seal the solution

Table 1: Average value of differences between absorbed doses from experimental measurement and estimates by DPM, MCNP, and EGSnrc MC codes for the single film setup. The standard deviation in the dose rate is calculated across repeat measurements for each film setup.

Experiment	Repeat measurements	Measurement Depth (mm)	Experiment Dose rate (µGy/GBq*s)	DPM vs Experiment (%)	MCNP vs Experiment (%)	EGSnrc vs Experiment (%)
Lu177$_{SF,S,25.4}$	4	0.2032	123.1 ± 4.1	-1.1	1.4	1.1
Lu177$_{SF,S,12.7}$	2	0.1651	153.3 ± 1.2	-0.6	1.7	1.3
Lu177$_{SF,B,25.4}$	3	0.2032	96.9 ± 1.2	-10.2	-6.8	-8.2
Y90$_{SF,S,25.4}$	4	0.2032	3495.3 ± 51.1	-1.2	0.0	0.1
Y90$_{SF,B,25.4}$	2	0.2032	2438.9 ± 26.8	-0.4	1.5	1.1

Table 1: Average value of differences between absorbed doses from experimental measurement and estimated by DPM, MCNP, and EGSnrc MC codes for the depth dose setup. The standard deviation in the dose rate is calculated across repeat measurements for each film depth.

Experiment	Repeat measurements	Depth (mm)	Experiment Dose rate (µGy/GBq*s)	DPM vs Experiment (%)	MCNP vs Experiment (%)	EGSnrc vs Experiment (%)
Lu177$_{DD,S,25.4}$	2	0.2032	132.1 ± 0.1	-8.0	-5.6	-5.9
		0.4812	23.6 ± 0.1	-3.5	1.3	0.3
		0.7592	8.9 ± 0.0	1.6	3.2	5.9
		1.0372	7.2 ± 0.2	5.6	7.6	9.1
		1.3152	6.6 ± 0.4	10.5	9.4	14.0
Y90$_{DD,S,25.4}$	3	0.2032	3371.2 ± 237.6	2.2	3.4	3.5
		0.4812	2601.4 ± 102.3	2.6	3.7	3.8
		0.7592	2050.9 ± 34.4	2.7	4.0	4.0
		1.0372	1614.3 ± 34.2	3.8	5.3	5.0
		1.3152	1290.7 ± 25.8	3.2	4.8	4.4
		1.5932	983.5 ± 24.5	7.6	9.4	8.6
		1.8712	791.1 ± 16.3	5.8	7.5	6.6
		2.1492	626.2 ± 20.7	4.9	6.9	5.4
		2.4272	483.7 ± 11.5	5.6	8.0	6.2
		2.7052	384.4 ± 14.3	1.8	5.3	3.4

Table A1: Sensitivity analysis for Capintec dose calibrators for Y-90 syringe activity measurements

	Dose Calibrator Setting					
	45	48	51	55	59	62
Capintec 15	0.43	0.43	0.42	0.41	0.39	0.38
Capintec 55	0.43	0.419	0.411	0.398	0.388	0.378
Capintec 55	0.413	0.404	0.395	0.383	0.373	0.363

Table A2: Measured variation in EBT3 film layer thicknesses. Values averaged over 3 different films with 3 positions measured for each variable.

	Measured Thickness (μm)	Manufacturer Specification (μm)	DPM Voxelized Thicknesses (μm)	% Difference MC Modeled Thickness vs Measured Thickness
Base	128.0	125.0	127	0.78
Active	25.1	28.0	25.4	1.19
Total	281.8	278.0	279.4	0.85

Table A3: Measured variation in Kapton tape with silicone adhesive. Values averaged over 2 different films with 3 positions measured for each thickness.

	Measured Thickness (µm)	Manufacturer Specification (µm)	DPM Voxelized Thicknesses (µm)	% Difference MC Modeled Thickness vs Measured Thickness
25.4µm Kapton	60.4	63.5	63.5	5.13
12.7µm Kapton	26.4	25.4	25.4	3.79

Table A4: Measured variation in 3D printed phantom thicknesses. Values averaged over 3 different phantoms with 3 positions measured for each variable.

	Measured (mm)	Designed (mm)	% Difference
Radial Depth	20.503	20.358	0.71
Wall Thickness	3.318	3.000	10.61
Top Thickness	11.861	11.500	3.13
Base Thickness	3.969	4.000	0.78

Table A5: Simulation materials and densities

Material	Density (g/cc)	Element	Atomic Fraction
Water	0.998	H	0.333
		O	0.666
Polyester Film Base	1.20	H	0.364
		C	0.455
		O	0.182
Active Film Layer	1.35	H	0.568
		Li	0.006
		C	0.276
		O	0.133
		Al	0.016
Kapton Polyimide Film	1.42	H	0.256
		C	0.564
		N	0.051
		O	0.128
Kapton Adhesive (Rubber, Silicon)	1.02	H	0.597
		C	0.199
		O	0.104
		Si	0.099
Liquid Bone	1.55	H	0.509
		O	0.382
		P	0.036
		K	0.073